Hydrophobic Cluster Formation Is Necessary for Dibenzofuran-Based Amino Acids to Function as β-Sheet Nucleators

Kwok Yin Tsang, Humberto Diaz, Nilsa Graciani, and Jeffery W. Kelly*

Contribution from the Department of Chemistry, Texas A&M University, College Station, Texas 77843-3255

Received August 12, 1993®

Abstract: Three dibenzofuran-based amino acid residues, namely 4-(2-aminoethyl)-6-dibenzofuranpropanoic acid (**1**), 4-(aminomethyl)-6-dibenzofuranethanoic acid (**2**), and 4-amino-6-dibenzofuranmethanoic acid (**3**), were prepared in order to compare their physical properties so as to further understand residue **1**'s ability to nucleate antiparallel β-sheet formation within small peptides in aqueous solution. FT-IR, variable temperature NMR, and an X-ray crystallography study reveal that amide analogs of **1** and **2** can adopt intramolecularly hydrogen bonded conformations in nonpolar solvents, whereas amides composed of residue **3** cannot. Spectroscopic studies reveal that linear heptapeptides containing **1** are capable of adopting a dynamic antiparallel β-sheet structure in aqueous solution, whereas residues **2** and **3** are incapable of nucleating a β-sheet structure in an otherwise identical peptide sequence. The efficacy of residue **1** as a β-sheet nucleator appears to result from a 15-membered ring intramolecularly hydrogen-bonded hydrophobic cluster conformation which serves as a partial β-sheet template enabling neighboring residues to be added to the growing sheet with a favorable equilibrium constant. The hydrophobic cluster conformation in these heptapeptides is stabilized by the interactions between the dibenzofuran skeleton in **1** and the hydrophobic side chains of the α-amino acid residues flanking **1**. In order for residue **1** to nucleate a β-sheet structure, it must be flanked with hydrophobic α-amino acid residues. Therefore, it is the tripeptide sequence—hydrophobic residue–**1**–hydrophobic residue—which mediates β-sheet nucleation. Residues **2** and **3** are not capable of promoting hydrophobic cluster formation, which apparently precludes these residues from being effective β-sheet nucleators, even though residue **2** facilitates intramolecular hydrogen bonding capable of supporting an antiparallel β-sheet structure. Spectroscopic methods for characterizing the hydrophobic cluster and the resulting β-sheet structure are described within.

Our comprehension of β-sheet structure in peptides and proteins is less clear than that of α-helical secondary structure, largely because a reliable isolated β-sheet model system has proven elusive.[1] Our understanding of the sequence required to afford an intramolecularly folded β-sheet is currently not sufficient for the *de novo* design of well-defined β-sheet structures.[2] The majority of what is known about β-sheet structure has resulted from studying the conformational propensities of homopolymers and sequential copolymers composed of one or two different amino acid residues, respectively.[3] However, polypeptides of this type are of limited utility because they form soluble β-sheets through self-association instead of, or in addition to, intramolecular folding.[3e-g] Employing small peptides to study sheet structure has proven difficult because of their propensity to self-associate into large, generally insoluble, quaternary β-sheet structures, with a few exceptions.[3f,4]

The mechanism(s) of β-sheet folding is (are) still not understood due to the lack of a good model system to test theoretical predictions.[5] Conversely, in the folding of α-helices, it is established that the initiation (nucleation) of an α-helix from a random coil conformation is the slowest and energetically most costly step.[6] Nucleation is thermodynamically unfavorable because of the conformational entropy penalty associated with fixing the dihedral angles in the three residues intervening between residues i and $i + 4$, which must be hydrogen bonded in order to form a core structure which facilitates helix propagation. Subsequent growth of the helix is rapid and thermodynamically favored because of the effective concentration of hydrogen-bonding donors and acceptors in the residues proximal to the nucleus and because the dihedral angles in only one residue need to be restricted in order to add that residue to the helix. Karplus and Mattice have recently published theoretical papers on β-sheet folding which predict that sheets could form from a nucleus of a partial β-sheet formed in an energetically unfavorable nucleation step.[5] Because of the difficulties in choosing a natural α-amino

® Abstract published in *Advance ACS Abstracts*, April 1, 1994.

(1) (a) Creighton, T. E. *Proteins: Structure and Molecular Properties*, 2nd ed.; W. H. Freeman and Co.: New York, 1993; pp 187. For recent progress in the development of small well-defined β-sheet model systems, see: (b) Kim, C. A.; Berg, J. M. *Nature* **1993**, *362*, 267. (c) Kemp, D. S.; Bowen, B. R. *Tetrahedron Lett.* **1988**, *29*, 5077. (d) Kemp, D. S.; Bowen, B. R.; Muendel, C.C. *J. Org. Chem.* **1990**, *55*, 4650. (e) Mutter, M.; Altmann, E.; Altmann, K.-H.; Hersperger, R.; Koziej, P.; Nebel, K.; Tuchscherer, G.; Vuilleumier, S.; Gremlich, H.-U.; Müller, K. *Helv. Chim. Acta.* **1988**, *71*, 835.

(2) Several small peptides are capable of populating a β-turn conformation, see: (a) Rose, G. D.; Gierasch, L. M.; Smith, J. A. *Adv. Protein Chem.* **1985**, *17*, 1. (b) Rizo, J.; Gierasch, L. M. *Annu. Rev. Biochem.* **1992**, *61*, 387. (c) Dyson, H. J.; Cross, K. J.; Houghten, R. A.; Wilson, I. A.; Wright, P. E.; Lerner, R. A. *Nature* **1985**, *318*, 480. However, only recently has it been shown that small peptides can form the more complex β-hairpin structure, see: (d) Blanco, F. J.; Jiménez, M. A.; Herranz, J.; Rico, M.; Santoro, J.; Nieto, J. L. *J. Am. Chem. Soc.* **1993**, *115*, 5887.

(3) (a) Maeda, H.; Ooi, K. *Biopolymers* **1981**, *20*, 1549. (b) Maeda, H. *Bull. Chem. Soc. Jpn.* **1987**, *60*, 3438. (c) Mattice, W. L. *Macromolecules* **1973**, *6*, 855. (d) Sarkar, P. K.; Doty, P. *Proc. Natl. Acad. Sci. U.S.A.* **1966**, *55*, 901. (e) Hartman, R.; Schwaner, R. C.; Hermans, J. *J. Mol. Biol.* **1974**, *90*, 415. (f) Brack, A.; Orgel, L. E. *Nature* **1975**, *256*, 383. (g) Brack, A.; Caille, A. *Int. J. Pep. Protein Res.* **1978**, *11*, 128. (h) Seipke, G.; Arfmann, H.-A. *Biopolymers* **1974**, *13*, 1621.

(4) (a) Degrado, W. F.; Lear, J. D. *J. Am. Chem. Soc.* **1985**, *107*, 7684. (b) Bode, K.; Goodman, M. *Helv. Chim. Acta* **1985**, *68*, 705. (c) Osterman, D.; Mora, R.; Kezdy, F. J.; Kaiser, E. T.; Meredith, S. C. *J. Am. Chem. Soc.* **1984**, *106*, 6845. (d) Osterman, D. G.; Kaiser, E. T. *J. Cell. Biochem.* **1985**, *29*, 57. (e) Altmann, K. H.; Florsheimer, A.; Mutter, M. *Int. J. Peptide Protein Res.* **1986**, *27*, 314. (f) Brack, A.; Caille, A. *Int. J. Peptide Protein Res.* **1978**, *11*, 128. (g) Rajasekharan Pillai, V. N.; Mutter, M. *Acc. Chem. Res.* **1981**, *14*, 122. (h) Mutter, M.; Gassmann, R.; Buttkus, U.; Altmann, K.-H. *Angew. Chem., Int. Ed. Engl.* **1991**, *30*, 1514. Also see refs 1b-e and 3f.

(5) (a) Yapa, K.; Weaver, D. L.; Karplus, M. *Proteins: Struct., Funct., Genet.* **1992**, *12*, 237. (b) Mattice, W. L. *Annu. Rev. Biophys. Biophys. Chem.* **1989**, *18*, 93.

(6) (a) Zimm, B. H.; Bragg, J. *J. Chem. Phys.* **1959**, *31*, 526. (b) Poland, D.; Scheraga, H. A. *Theory of Helix-Coil Transitions in Biopolymers*; Academic Press: New York, 1970.

0002-7863/94/1516-3988$04.50/0 © 1994 American Chemical Society

acid sequence which will adopt a partial β-sheet structure capable of nucleating a β-sheet,[2,7] we set out to design an amino acid that will stabilize a partial β-sheet structure and thus nucleate β-sheet formation in aqueous solution.[8]

The concept of introducing a conformationally rigid molecule into a peptide to stabilize a single conformation was established by Hirschmann, Veber, Freidinger, Nutt, and their colleagues at Merck.[9] Since then and previous to our efforts, several elegant dipeptide and related β-turn mimetics have been prepared either to control the conformation of peptides and/or as potential pharmaceuticals.[10] The ability to design a molecular fragment which nucleates β-sheet formation was first demonstrated by Kemp by employing the epindolidione nucleus. When the epindolidione ring system is incorporated into an α-amino acid sequence, it serves as an artificial β-strand and mediates sheet formation via hydrogen bonding between the epindolidione skeleton and the covalently attached peptide chain.[1c,d,11] The goal of the work described here is to develop an amino acid that is a dipeptide mimetic of the $i + 1$ and $i + 2$ residues of a β-turn in an effort to nucleate β-sheet folding without significantly perturbing the resulting antiparallel β-sheet structure. Protein folding is driven by the hydrophobic effect and opposed by the local and nonlocal conformational entropy of the chain.[7,12] Our dipeptide mimetic (**1**) is designed to reverse the polypeptide chain with a minimal entropic penalty and promote hydrophobic cluster formation. The latter appears to be important for the nucleation of protein folding.[7,13] Rose and Dill have proposed that protein folding proceeds first through the formation of hydrophobic clusters, which direct the folding of the peptide chain into various low-energy secondary structures such as α-helices and β-sheets.[7] This proposal is gaining acceptance because of the recent NMR spectroscopic studies of Wuthrich and Dobson, who have shown that hydrophobic clusters exist in the "denatured state" of the 434 repressor and lysozyme, respectively.[13a,b] These hydrophobic clusters seem to nucleate the folding of those proteins. The fluorescence studies carried out by Matthews et al. on dihydrofolate reductase refolding also support this role for the hydrophobic cluster.[13c] They have evidence that a hydrophobic cluster forms during the early stages of dihydrofolate reductase folding. Hydrophobic clusters also appear to be important for stabilizing the active conformation of peptides including somatostatin and cyclosporine.[10c,e] In summary, residue **1** has been designed to minimize the chain entropy penalty associated with β-sheet folding and maximize hydrophobic interactions such that the hydrophobic cluster mediates antiparallel β-sheet folding.

Dibenzofuran was chosen as the backbone of the nucleating amino acid because the distance between C4 and C6 (4.9 Å) is very close to the distance between the strands of an antiparallel β-sheet (4.85 Å).[14] Aminoethyl and carboxyethyl functionalizations at C4 and C6 of dibenzofuran were selected because studies on the conformation of phenethylamine and other related derivatives in a variety of solvents have shown that the low energy conformer is that which positions the aliphatic carbon–carbon bond perpendicular to the plane of the aromatic ring (Figure 1).[15] The perpendicular conformation of the dibenzofuran-based amino acid 4-(2-aminoethyl)-6-dibenzofuranpropanoic acid (**1**) is desirable for nucleating β-sheet structure in water for two reasons. First, the perpendicular conformation is sufficient to reverse the polypeptide chain direction while maintaining a hydrogen bond between the α-amino acid residues flanking **1**, which is important for reducing the conformational entropy penalty associated with nucleation. Secondly, the perpendicular conformation facilitates a hydrophobic interaction between the dibenzofuran skeleton and the hydrophobic side chains of the α-amino acid residues flanking **1** (Figure 1B,C). In addition to nucleating sheet formation, the hydrophobic cluster may also stabilize the folded antiparallel β-sheet over the unfolded state if the cluster is less solvated when the peptide is fully folded.

The preparations of nucleator **1**[8a] and two additional dibenzofuran-based amino acids, namely 4-(aminomethyl)-6-dibenzofuranethanoic acid (**2**) and 4-amino-6-dibenzofuranmethanoic acid (**3**), are described within. Residues **1**, **2**, and **3** differ with respect to the aliphatic linkage which intervenes between the dibenzofuran skeleton and the amide functionalities (Figure 2). Amino acids **2** and **3** were prepared in order to compare their physical properties to those of **1** in an attempt to further understand **1**'s ability to nucleate β-sheet structure, which was communicated previously.[8d] The abilities of simple amide derivatives of **2** and **3** to undergo intramolecular hydrogen bonding were compared with those derived from **1** by employing variable-temperature NMR and FT-IR studies in CH_2Cl_2.[8b,c] Methylene chloride was chosen as a solvent to make conditions ideal for intramolecular hydrogen bonding because CH_2Cl_2 cannot readily serve as a hydrogen bond donor or acceptor. If an amide derivative of **1**, **2**, or **3** forms an intramolecular hydrogen bond in CH_2Cl_2, it will

(7) Designing a small peptide which will form a hydrophobic cluster and adopt an intramolecular β-sheet structure should be possible but has not been realized yet. For a discussion of the importance of hydrophobic clusters and collapse in protein folding, see: (a) Kauzmann, W. *Adv. Protein Chem.* **1959**, *14*, 1. (b) Rose, G. D.; Roy, S. *Proc. Natl. Acad. Sci. U.S.A.* **1980**, *77*, 4643. (c) Dill, K.A.; Chan, H. S. *Proc. Natl. Acad. Sci. U.S.A.* **1990**, *87*, 6388. For a demonstration of the importance of hydrogen bonding in β-sheet formation, see: (d) Blake, C. C. F.; Geisow, M. J.; Oatley, S. J. *J. Mol. Biol.* **1978**, *121*, 339 and references within.

(8) (a) Díaz, H.; Kelly, J. W. *Tetrahedron Lett.* **1991**, *41*, 5725. (b) Díaz, H.; Espina, J. R.; Kelly, J. W. *J. Am. Chem. Soc.* **1992**, *114*, 8316. (c) Díaz, H.; Tsang, K. Y.; Choo, D.; Kelly, J. W. *Tetrahedron* **1993**, *49*, 3533. (d) Díaz, H.; Tsang, K. Y.; Choo, D.; Espina, J. R.; Kelly, J. W. *J. Am. Chem. Soc.* **1993**, *115*, 3790.

(9) (a) Veber, D. F.; Strachan, R. G.; Bergstrand, S. J.; Holly, F. W.; Homnick, C.F.; Hirschmann, R. *J. Am. Chem. Soc.* **1976**, *98*, 2367. (b) Veber, D. F.; Holly, F. W.; Palveda, W. J.; Nutt, R. F.; Bergstrand, S. J.; Torchiana, M.; Glitzer, M. S.; Saperstein, R.; Hirschmann, R. *Proc. Natl. Acad. Sci. U.S.A.* **1978**, *75*, 2636. (c) Veber, D. F.; Saperstein, R.; Nutt, R. F.; Freidinger, R. M.; Brady, S. F.; Curley, P.; Perlow, D. S.; Palveda, W. J.; Colton, C. D.; Zacchei, A. G.; Toco, D. J.; Hoff, D. R.; Vandlen, R. L.; Gerich, J. E.; Hall, L.; Mandarino, L.; Cordes, E. H.; Anderson, P. S.; Hirschmann, R. *Life Sci.* **1984**, *34*, 1371. (d) Freidinger, R. M.; Veber, D. F.; Schwenk Perlow, D. *Science* **1980**, *210*, 656.

(10) For reviews (a-h) and references related to the design, synthesis, and evaluation of β-turn mimetics see: (a) Hölzemann, G. *Kontakte (Darmstadt)* **1991**, 3. (b) Hölzemann, G. *Kontakte (Darmstadt)* **1991**, 55. (c) Hirschmann, R. *Angew. Chem., Int. Ed. Engl.* **1991**, *30*, 1278. (d) Olson, G. L.; Bolin, D. R.; Bonner, M. P.; Bös, M.; Cook, C. M.; Fry, D. C.; Graves, B. J.; Hatada, M.; Hill, D. E.; Kahn, M.; Madison, V. S.; Rusiecki, V. K.; Sarabu, R.; Sepinwall, J.; Vincent, G. P.; Voss, M. E. *J. Med. Chem.* **1993**, *36*, 3039. (e) Wiley, R. A.; Rich, D. H. *Med. Res. Rev.* **1993**, *13*, 327. (f) Freidinger, R. M. *Trends Pharmacol. Sci.* **1989**, *10*, 270. (g) Goodman, M.; Ro, S. *Burger's Medicinal Chemistry and Drug Discovery*, 5th ed., Volume 1 (Principles of Drug Discovery), in press. (h) Kahn, M. *Synlett* **1993**, 821. (i) Ernest, I.; Kalvoda, J.; Rihs, G.; Mutter, M. *Tetrahedron Lett.* **1990**, *31*, 4011. (j) Kemp, D. S.; Bowen, B. R.; Muendel, C. C. *J. Org. Chem.* **1990**, *55*, 4650. (k) Olson, G. L.; Voss, M. E.; Hill, D. E.; Kahn, M.; Madison, V. S.; Cook, C. M. *J. Am. Chem. Soc.* **1990**, *112*, 323. (l) Brandmeier, V.; Feigel, M. *Tetrahedron* **1989**, *45*, 1365. (m) Feigel, M. *Liebigs Ann. Chem.* **1989**, 459. (n) Kahn, M.; Bertenshaw, C. M. *Tetrahedron Lett.* **1989**, *30*, 2317. (o) Kahn, M.; Wilke, S.; Chen, B.; Fujita, K. *J. Am. Chem. Soc.* **1988**, *110*, 1638. (p) Kemp, D. S.; Bowen, B. R. *Tetrahedron Lett.* **1988**, *29*, 5077. (q) Kemp, D. S.; Stites, W. E. *Tetrahedron Lett.* **1988**, *29*, 5057. (r) Kahn, M.; Chen, C. M. *Tetrahedron Lett.* **1987**, *28*, 1623. (s) Feigel, M. *J. Am. Chem. Soc.* **1986**, *108*, 181. (t) Kahn, M.; Devens, B. *Tetrahedron Lett.* **1986**, *27*, 4841. (u) Sato, K.; Nagai, U. *J. Chem. Soc., Perkin. Trans. 1* **1986**, 1231. (v) Kemp, D. S.; McNamara, P. E. *J. Org. Chem.* **1985**, *50*, 5834. (w) Nagai, U.; Sato, K. *Tetrahedron Lett.* **1985**, *26*, 647. (x) Kemp, D. S.; McNamara, P. E. *J. Org. Chem.* **1984**, *49*, 2286. (y) Kemp, D. S.; Sun, E. T. *Tetrahedron Lett.* **1982**, *23*, 3759. (z) Krstenansky, J. L.; Baranowski, R. L.; Currie, R. L. *Biochem. Biophys. Res. Commun.* **1982**, *109*, 1368. (aa) Hinds, M. G.; Richards, N. G. J.; Robinson, J.A. *J. Chem Soc., Chem. Commun.* **1988**, 1447. (bb) Nowick, J. S.; Powell, N.A.; Martinez, E. J.; Smith, E. M.; Noronha, G. *J. Org. Chem.* **1992**, *57*, 3763.

(11) (a) Kemp, D. S.; Bowen, B. R. *Tetrahedron Lett.* **1988**, *29*, 5081. (b) Kemp, D. S. *Trends Biotechnol.* **1990**, *6*, 246.

(12) (a) Dill, K. A. *Biochemistry* **1990**, *29*, 7133. (b) Tanford, C. *The Hydrophobic Effect*; Wiley and Sons: New York, 1973; pp 200.

(13) (a) Neri, D.; Billeter, G.; Wider, G.; Wuthrich, K. *Science* **1992**, *257*, 1559. (b) Topping, K. D.; Evans, P. A.; Dobson, C. M. *Proteins* **1991**, *9*, 246. (c) Garvey, E. P.; Swank, J.; Matthews, C. R. *Proteins* **1989**, *6*, 259.

(14) (a) Pauling, L.; Corey, R. B. *Proc. Natl. Acad. Sci.* **1953**, *39*, 253. (b) Reppart, W. J.; Gallucci, J. C.; Lundstedt, A. P.; Gerkin, R. E. *Acta Cryst.* **1984**, *C40*, 1572.

(15) (a) Scharfenberg, P.; Rozsondai, B.; Hargittai, I. *Z. Naturforsch., A* **1980**, *35a*, 431. (b) Kriz, J.; Jakes, J. *J. Mol. Struct.* **1972**, *12*, 367.

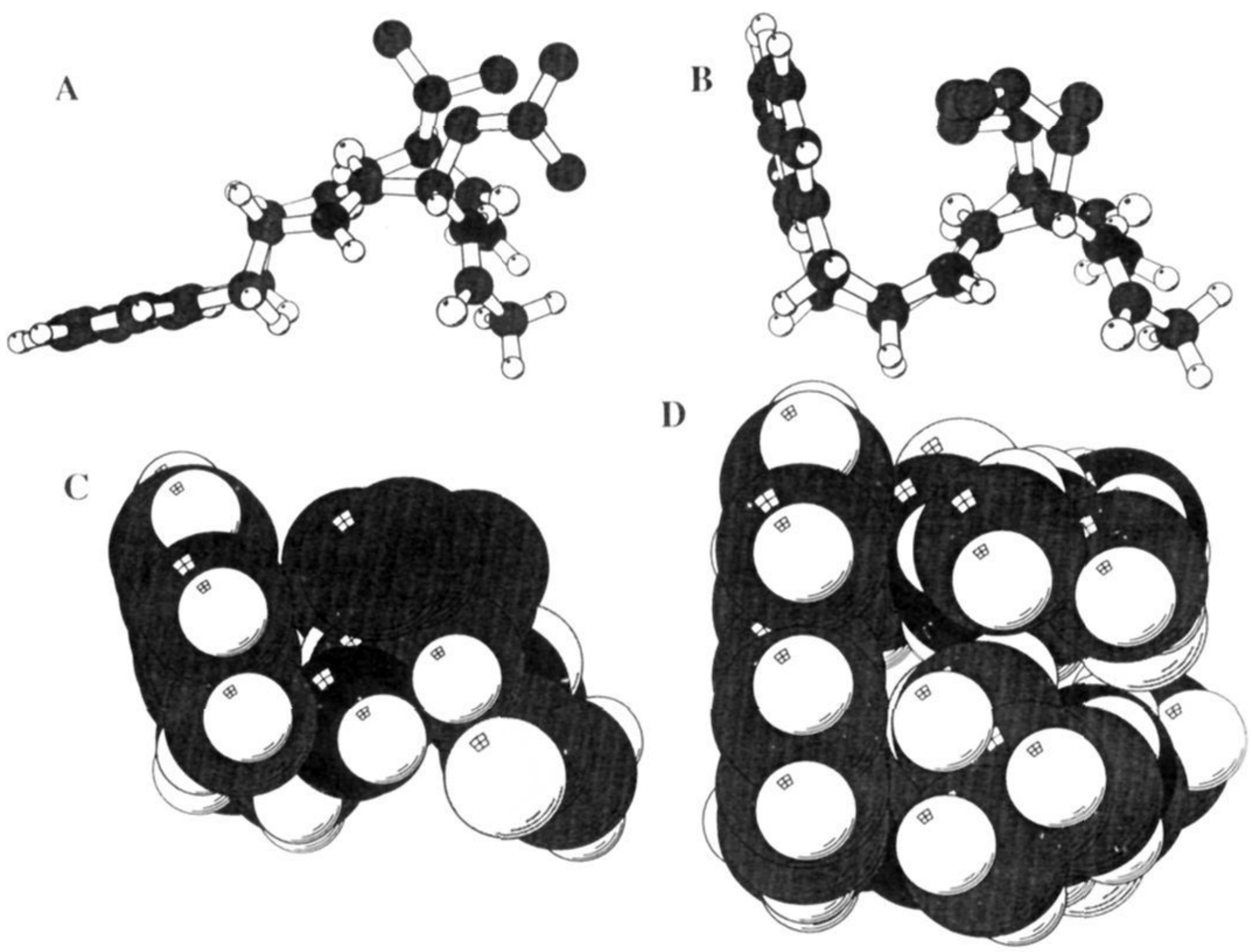

Figure 1. Molecular Graphics depiction[36] of Ac-Leu-**1**-Val-NH_2 demonstrating the two conformational states that residue **1** can adopt (see Figure 2 for a line drawing of **1**). Structure A illustrates the lowest energy extended conformation adopted by residue **1** within a peptide in a nonpolar environment as discerned by molecular mechanics/molecular dynamics and by X-ray crystallography (see Figure 9). This extended conformation is also observed in aqueous solution in peptides when the α-amino acid residues flanking **1** are not hydrophobic residues (see text). Structure A is oriented such that the dibenzofuran skeleton and the hydrogen bonds between the α-amino acid residues flanking **1** are perpendicular to the plane of the page; the H's have been left off the α-amino acid side chains for clarity. Note the perpendicular conformation of the alkyl portion of **1** relative to the aromatic skeleton (see text). Structure B illustrates the alternative hydrophobic cluster conformation adopted by **1** in aqueous solution. The hydrophobic cluster conformation of **1** is only slightly higher in energy than the extended conformation in nonpolar solvents. The hydrophobic cluster conformation is stabilized by hydrophobic interactions between the dibenzofuran skeleton and the side chains of the flanking α-amino acid residues in aqueous solution, as demonstrated by NOESY-NMR and near-UV CD studies described within. All indications are that the hydrophobic effect stabilizes the hydrophobic cluster conformation of **1** in aqueous solution such that it is the predominant conformer. Note that the alkyl C–C bonds in **1** are still perpendicular to the plane of the dibenzofuran skeleton in the hydrophobic cluster conformation (H's have been deleted from the α-amino acid side chains for clarity). A CPK representation of the hydrophobic cluster conformation B is shown in Figure 1C. Note that the van der Waals surfaces of the dibenzofuran skeleton and the isobutyl group of the flanking leucine residue pack tightly to form a hydrophobic cluster or core (H's have been left off the α-amino acid side chains for clarity). An alternative CPK view of the hydrophobic cluster conformation is shown in structure D. In this view the reader is looking down onto the hydrophobic cluster such that the hydrogen bonds between the Leu and Val α-amino acid residues are in the plane of the page (but are not visible). This view clearly shows the ideal hydrophobic interactions between the dibenzofuran skeleton and the Leu and Val side chains (side chain H's are shown here).

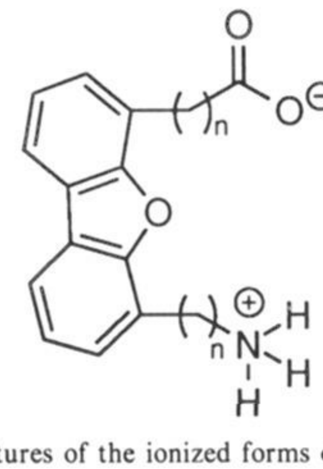

Figure 2. Structures of the ionized forms of amino acids **1**, **2**, and **3**.

be assumed that it also has the potential to do so in aqueous solution. This assumption is reasonable if the hydrogen bond in question is protected from solvent by the secondary structure adopted in water. Finally, residues **1**, **2**, and **3** were incorporated into identical heptapeptides to probe their ability to nucleate a β-sheet structure in aqueous solution and to probe the sequence requirements for β-sheet nucleation. Spectroscopic studies indicate that residue **1** is an effective nucleator because it promotes hydrophobic cluster formation in addition to intramolecular hydrogen bonding. Residues **2** and **3** cannot form an intramolecularly hydrogen-bonded hydrophobic cluster, which likely explains why these residues cannot nucleate β-sheet structure in aqueous solution. Several heptapeptides incorporating **1** which have sequence variability at the flanking positions were prepared in order to focus on the sequence requirements for β-sheet nucleation.

Results

Synthesis of β-Turn Mimics 1, 2, and 3. The synthesis of **1**, **2**, and **3** employ a common intermediate, namely 4,6-diiododibenzofuran (**4**) (Figure 3). This intermediate was prepared by treating dibenzofuran with *sec*-butyllithium and TMEDA in diethyl ether at –78 °C to afford 4,6-bis-lithiated dibenzofuran. Addition of iodine to the dianion yields 4,6-diiododibenzofuran (**4**) in 83% yield.[16] The synthesis of a Boc-protected C-terminally activated analog of 4-(2-aminoethyl)-6-dibenzofuranpropanoic acid (**1**), as outlined in Figure 3, begins by subjecting **4** to a palladium catalyzed Heck cross-coupling reaction with ethyl acrylate to afford the bis-α,β-unsaturated ethyl ester **5** in 93% yield.[17] Saponification followed by hydrogenation yields the saturated C_2 symmetrical diacid **6** in 93% yield. The diacid is

(16) Benaksas Schwartz, E. J. Ph.D. Thesis, University of California, Los Angeles, 1989.

(17) (a) Ziegler, C. B.; Heck, R. F. *J. Org. Chem.* **1978**, *43*, 2941. (b) Heck, R. F. *Org. React.* **1982**, *27*, 345.

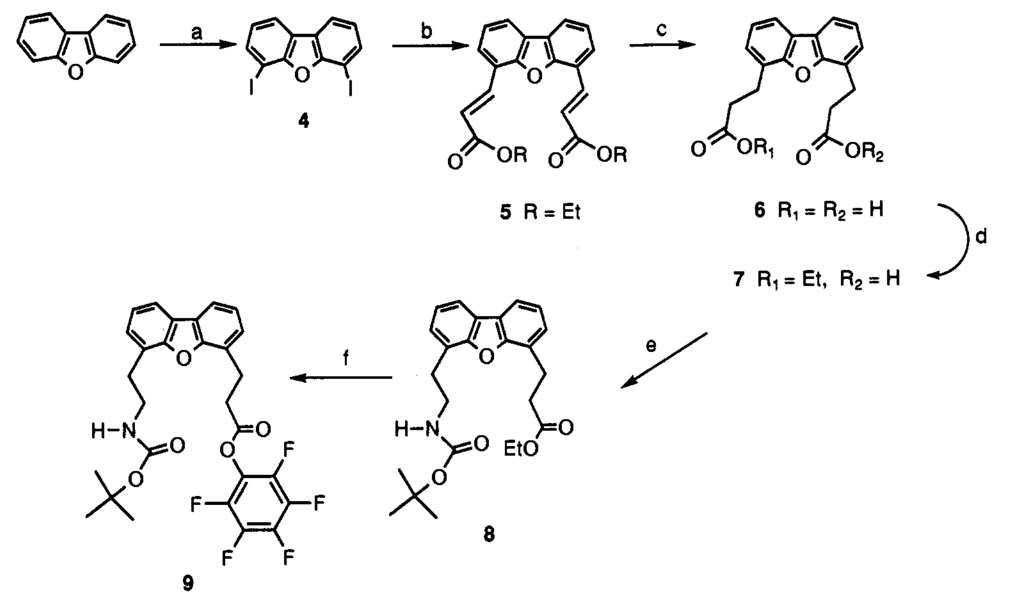

Figure 3. Outline of the synthesis of **9** (protected and activated form of amino acid **1**). Reaction conditions: (a) (i) 3 equiv of *s*-BuLi, 3 equiv of TMEDA, diethyl ether, initially at −78 °C and then allowed to warm to room temperature, 24 h, (ii) 4.6 equiv of I_2, diethyl ether, −78 °C, 12 h, 83%; (b) 2.5 equiv of ethyl acrylate, 0.1 equiv of tri-*o*-tolylphosphine, 0.02 equiv of palladium(II) acetate, DMF, 95–97 °C, 0.5 h, 93%; (c) (i) 1.5 equiv of NaOH, ethanol, reflux, 2 h, (ii) H_2, 10% Pd on activated carbon, H_2O, room temperature, 4 h, (iii) 2 N HCl, filtration, 93%; (d) ethanol, reflux, 50 h, 53%; (e) 1.2 equiv of diphenylphosphoric azide, 1 equiv of TEA, *tert*-butyl alcohol, reflux, 24 h, 75%; (f) (i) 1.5 equiv of NaOH, ethanol, reflux, 2 h, (ii) 1.1 equiv of pentafluorophenol, 1 equiv of DCC, ethyl acetate, initially at 0 °C and then allowed to warm to room temperature, 14 h, 88%.

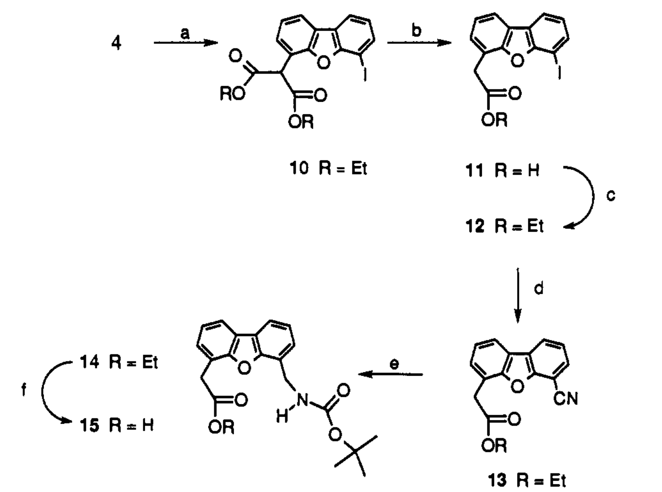

Figure 4. Outline of the synthesis of **15** (*t*-Boc-protected **2**). Reaction conditions: (a) 3 equiv of NaH, 3 equiv of diethyl malonate, 3 equiv of CuBr, dioxane, reflux, 2 h, 72%; (b) 1 N NaOH/ethanol (1:1), reflux, 2 h, 99%; (c) (i) 20 equiv of thionyl chloride, chloroform, reflux, 3 h, (ii) ethanol, reflux, 0.5 h, 98%; (d) 2.5 equiv of CuCN, DMF, reflux, 2.5 h, 99%; (e) (i) H_2, Raney nickel, NH_3/ethanol, room temperature, 2 days, (ii) 1.5 equiv of di-*tert*-butyl dicarbonate, THF, reflux, 2 h, 90 %; (f) 1 equiv NaOH, ethanol, reflux, 2 h, crude 99%.

converted to the monoester **7** by employing a self-catalyzed Fisher esterification reaction. The monoacid functionality in **7** is then converted to the *tert*-butyl carbamate **8** by employing a Schmidt rearrangement. Saponification of the ethyl ester in **8** followed by conversion of the carboxylic acid to the pentafluorophenyl active ester yields **9**, which was used directly in solid phase peptide synthesis and in the preparation of simple amides. The overall yield of **9** from dibenzofuran is 25%.

The synthesis of **15**, a Boc-protected analog of **2**, is outlined in Figure 4. The preparation commences with a reaction between the diiodide **4** and sodium diethyl malonate in the presence of copper(I) bromide which affords the mono diethyl malonate substituted dibenzofuran **10** as the major product in 72% yield.[18]

(18) Setsune, J.; Matsukawa, K.; Wakemoto, H.; Kitao, T. *Chem. Lett.* **1981**, 367.

Hydrolysis of **10** facilitates spontaneous decarboxylation, yielding the iodoacid **11**, which was converted to iodoester **12** by treatment with thionyl chloride and anhydrous ethanol. The cyanoester **13** was obtained in 99% yield by coupling **12** with copper(I) cyanide in DMF at 155 °C.[19] Catalytic hydrogenation of **13** employing a Raney nickel catalyst in ammonia-saturated ethanol[20] gave the corresponding amino ester which was treated with di-*tert*-butyl dicarbonate to afford the carbamate **14** in 90% yield. Saponification of ester **14** with KOH yields the Boc-protected amino acid **15**, which was utilized in solid-phase peptide synthesis and in the preparation of simple amides for FT-IR and NMR studies. The amino acid was stored as the ethyl ester **14** and hydrolyzed prior to use. The overall yield of **15** from dibenzofuran is 51%.

The synthesis of **21**, *t*-Boc protected **3**, is depicted in Figure 5. Coupling of the diiodide **4** with copper(I) cyanide in DMF at 155 °C yields 4,6-dicyanodibenzofuran (**16**) in 95% yield.[19] 4,6-Dicyanodibenzofuran was hydrolyzed to afford the diacid **17**, which was converted to the diester **18** by treating **17** with thionyl chloride and subsequently with absolute ethanol. The monoacid **19** was obtained by hydrolysis of diester **18** using 1 equiv of NaOH. Carbamate **20** was obtained from acid **19** in 79% yield by employing a Schmidt rearrangement using anhydrous *tert*-butyl alcohol as the solvent. Saponification of **20** with KOH affords the *t*-Boc-protected amino acid **21**, which was employed to make peptides and amide derivatives containing amino acid residue **3**. The overall yield of **21** from dibenzofuran is 24%.

Synthesis of Simple Amides for FT-IR and VT-NMR Studies. The ability of residues **1**, **2**, and **3** to promote intramolecular hydrogen bonding in simple amide derivatives in a noncompetitive solvent was evaluated by FT-IR and variable-temperature NMR spectroscopy.[8b,21] Figure 6 outlines the methodology used to

(19) (a) Patel, B. A.; Ziegler, C. B.; Cortese, N. A.; Plevyak, J. E.; Zebovitz, T. C.; Terpko, M.; Heck, R. F. *J. Org. Chem.* **1977**, *42*, 3903. (b) Hegedus, L. S.; Allen, G. F.; Bozell, J. J.; Waterman, E. L. *J. Am. Chem. Soc.* **1978**, *100*, 5800.

(20) Kita, Y.; Tohma, H.; Inagaki, M.; Hatanaka, K.; Yakura, T. *J. Am. Chem. Soc.* **1992**, *114*, 2175.

(21) (a) Stevens, E. S.; Sugawara, N.; Bonora, G. M.; Toniolo, C. *J. Am. Chem. Soc.* **1980**, *102*, 7048. (b) Gellman, S. H.; Adams, B. R.; Dado, G. P. *J. Am. Chem. Soc.* **1990**, *112*, 460. (c) Gellman, S. H.; Dado, G. P.; Liang, G.; Adams, B. R. *J. Am. Chem. Soc.* **1991**, *113*, 1164. (d) Liang, G.; Dado, G. P.; Gellman, S. H. *J. Am. Chem. Soc.* **1991**, *113*, 3994. (e) Liang, G.; Rito, C. J.; Gellman, S. H. *J. Am. Chem. Soc.* **1992**, *114*, 4440.

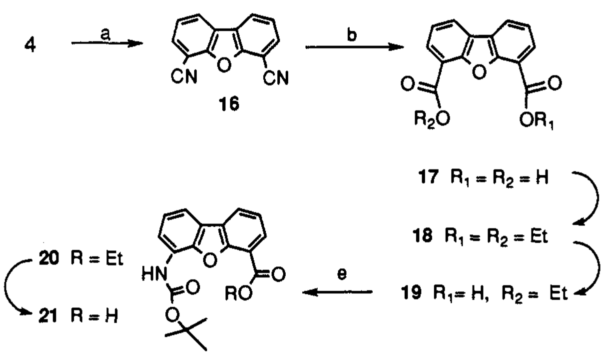

Figure 5. Outline of the synthesis of **21** (*t*-Boc protected **3**). Reaction conditions: (a) 4 equiv of CuCN, DMF, reflux, 2 h, 95%; (b) 1 N NaOH/methanol (1:1), reflux, 24 h, 99%; (c) (i) 30 equiv of thionyl chloride, chloroform, reflux, 3 h, (ii) ethanol, reflux, 1 h, 97%; (d) 1 equiv of NaOH, ethanol, reflux, 2 h, 40%; (e) 1.2 equiv of diphenylphosphoric azide, 1 equiv of TEA, *tert*-butyl alcohol, reflux, 24 h, 79 %; (*f*) 1 equiv of NaOH, ethanol, reflux, 2 h, crude 99%.

prepare simple amide derivatives of amino acids **1**, **2**, and **3** for the IR and NMR studies. Removal of ethyl ester protecting groups in **14** and **20** was accomplished by basic hydrolysis, affording the *tert*-butyloxycarbonyl- (*t*-Boc-) protected amino acids **15** and **21**, respectively. Conversion of the acid functionality to an amide derived from isobutylamine or diethylamine was achieved using BOP activation. Amide analogs of **1**, i.e. **22** and **23**, were prepared by amine displacement of the pentafluorophenoxy group in **9**. The *t*-Boc protecting groups were then removed in compounds **22-26** using a 25–50% TFA solution in dichloromethane. Excess TFA was eliminated by treating the crude product with Amberlyst A-21. Acetylation of the free amino group with acetic anhydride gave the corresponding diamides **27-31**. Amide **32** was synthesized using a similar strategy but without hydrolysis of the ethyl ester group in **14**. Imide analogs **35** and **36** were prepared by removing the *t*-Boc protecting group in **24** and **22** with TFA. The amino amides were then treated with an excess of succinic anhydride to afford **33** and **34**. Cyclization of the amidic acids was achieved using acetic anhydride and sodium acetate to afford **35** and **36**. No purification was carried out on any of the intermediates shown in Figure 6, however, the final products were purified by reverse-phase HPLC, affording 50–95% yields of the expected amide analogs of **1**, **2**, and **3**. All amides were dried over NaOH under high vacuum for extended periods to ensure removal of TFA, which was verified by FT-IR analysis of the amides.

FT-IR Studies. The presence of intramolecular amide–amide hydrogen bonding was probed by analyzing the amide N-H IR stretch region (3200–3500 cm^{-1}). A sharp signal at 3400–3500 cm^{-1} in CH_2Cl_2 usually corresponds to a free N-H, whereas an amide hydrogen bonded N-H results in a broader infrared band absorbing from ≈3200–3400 cm^{-1}.[21] We have previously established that intermolecular amide–amide hydrogen bonding is not detectable in 1.5 mM solutions of dibenzofuran-based amides.[8b] Therefore, the observed spectra result only from intramolecular hydrogen bonding or lack thereof.[8b,21] A previous infrared study on amides **27** and **28** and related analogs derived from amino acid **1** reveals that the 15-membered intramolecularly hydrogen-bonded conformer shown in eq 1 (**27a**) is observed at room temperature in CH_2Cl_2 (Figure 7a). The alternative 13-membered intramolecularly hydrogen bonded amide is not observed (**27b**), even in cases where it is impossible to form a 15-membered intramolecularly hydrogen-bonded conformer, e.g. amide **28** (Figures 6 and 7b).[8b] The 15-membered ring intramolecular hydrogen bond in amides composed of **1** is ideal for nucleating β-sheet formation because **1** replaces what would be residues $i + 1$ and $i + 2$ in a normal β-turn and facilitates an intramolecular hydrogen bond between what would be the i and $i + 3$ residues of a β-turn. The N—H and C=O of **1** do not

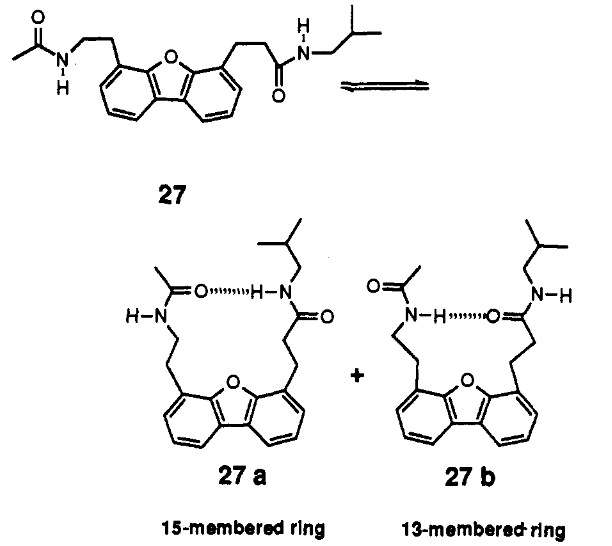

(1)

intramolecularly hydrogen bond; rather, the carbonyl and the N—H of the R-groups attached via an amide linkage to **1** intramolecularly hydrogen bond (eq 1, **27a**). We have previously shown by FT-IR that residue **1** can support a β-sheet-like hydrogen-bonding scheme where the residues flanking **1** are multiply intramolecularly hydrogen bonded in CH_2Cl_2.[8c] Computational studies suggest that the alternative 13-membered intramolecular hydrogen bond is not observed because it is destabilized by torsional strain.[8b]

Infrared studies of simple amides composed of the dibenzofuran-based amino acid **2** reveal that these amides, e.g. **29**, can intramolecularly hydrogen bond. The amide N—H stretch region of **29** reveals two bands with maxima at 3443 cm^{-1} (nonbonded N—H) and 3351 cm^{-1} (hydrogen bonded N—H) (Figure 7c). Inspection of CPK models of analog **29** suggests three possible intramolecularly hydrogen-bonded conformers (eq 2). These

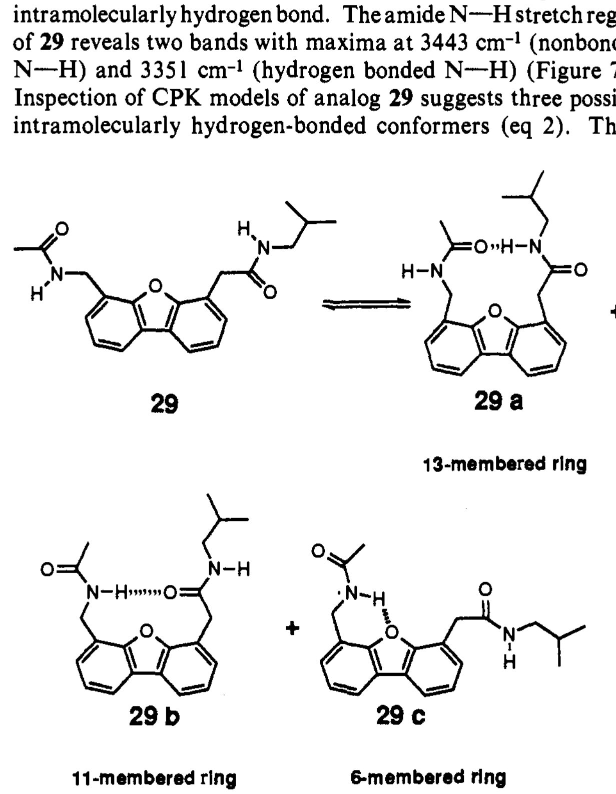

(2)

include rings having 13 (**29a**) or 11 members (**29b**) and less likely a six-membered ring (**29c**) where the dibenzofuran oxygen serves as the hydrogen bond acceptor. Since we found it difficult to establish whether **29a** or **29b** (or a combination thereof) is the favored hydrogen-bonded conformation, compound **30** was prepared. Replacement of the isobutylamide group in **29** by the diethylamide functionality yields **30**, which is incapable of adopting a 13-membered ring hydrogen-bonded conformation.

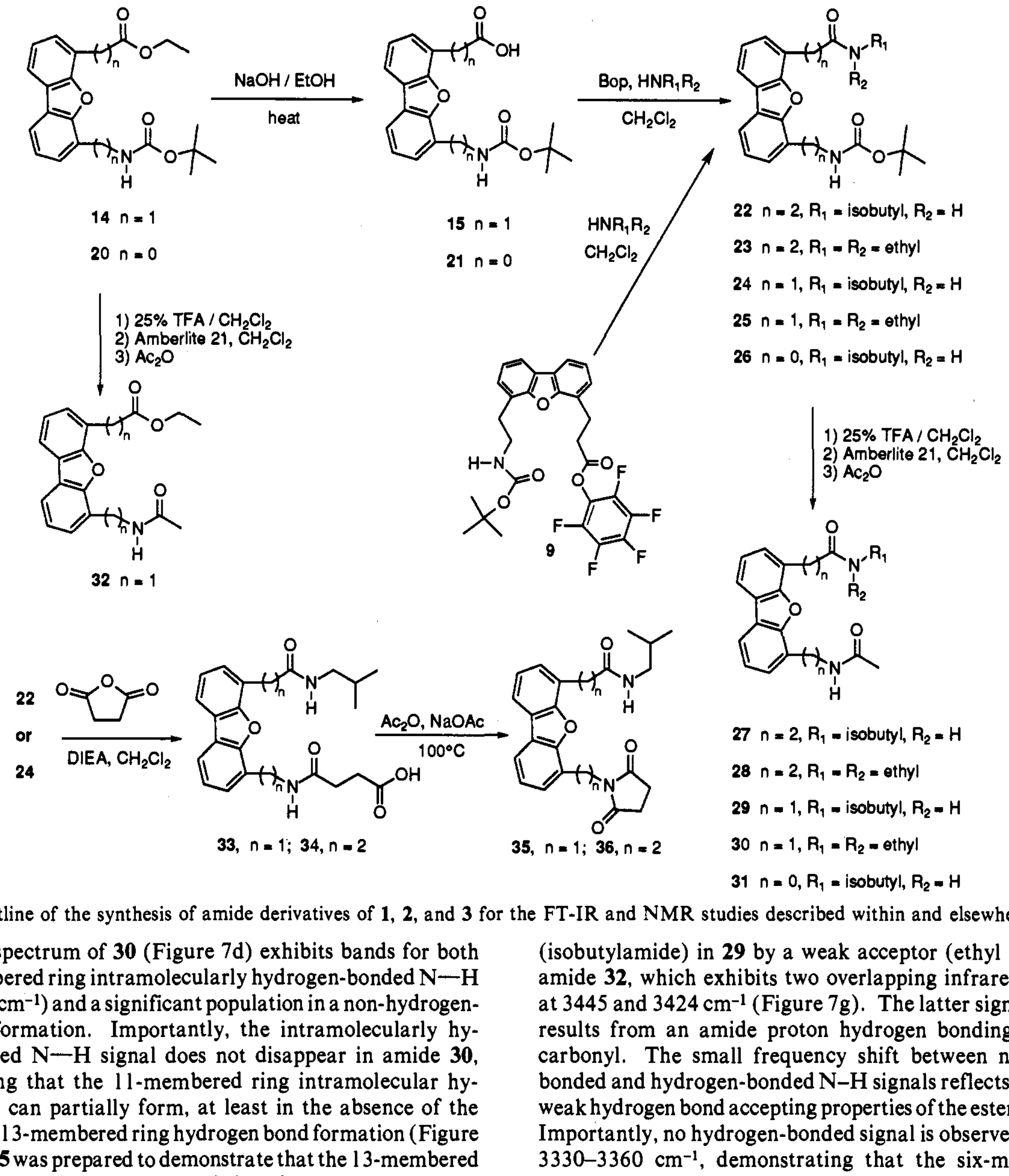

Figure 6. Outline of the synthesis of amide derivatives of **1**, **2**, and **3** for the FT-IR and NMR studies described within and elsewhere.[8b]

The FT-IR spectrum of **30** (Figure 7d) exhibits bands for both the 11-membered ring intramolecularly hydrogen-bonded N—H signal (3360 cm^{-1}) and a significant population in a non-hydrogen-bonded conformation. Importantly, the intramolecularly hydrogen-bonded N—H signal does not disappear in amide **30**, demonstrating that the 11-membered ring intramolecular hydrogen bond can partially form, at least in the absence of the possibility of 13-membered ring hydrogen bond formation (Figure 7d). Imide **35** was prepared to demonstrate that the 13-membered ring intramolecularly hydrogen-bonded conformation was a stable conformation and the one that is likely to predominate in amides such as **29**. Imide **35** is incapable of adopting an 11-membered ring intramolecularly hydrogen-bonded conformation. An infrared study on imide **35** reveals that it is nearly completely hydrogen bonded, implying that the 13-membered intramolecularly hydrogen-bonded conformer is the favored one in amide **29** in noncompetitive solvents (Figure 7e). This observation is especially relevant because the imide carbonyls in **35** are poorer hydrogen-bonding acceptors than the amide carbonyls in **29**, as evidenced by the decrease in the frequency shift between hydrogen-bonded (3396 cm^{-1}) and non-hydrogen-bonded (3444 cm^{-1}) amide N–H's. Interestingly, the FT-IR spectra of imide **35**, composed of **2**, and imide **36**, composed of **1**, are nearly identical (Figure 7, panels e and f, respectively), suggesting that the extent of 13-membered ring intramolecular hydrogen bonding in amides composed of **2** is comparable to the extent of 15-membered ring intramolecular hydrogen bonding observed in amides composed of **1**. The predominance of the 13-membered hydrogen-bonded conformer, **29a**, is also supported by the VT-NMR data described below. The ester amide **32** was synthesized to clarify the possible contribution of the six-membered ring intramolecular hydrogen bond in **29c** to the hydrogen-bonded IR signal exhibited by **29** and **30**. Replacement of the strong hydrogen bond acceptor (isobutylamide) in **29** by a weak acceptor (ethyl ester) affords amide **32**, which exhibits two overlapping infrared absorptions at 3445 and 3424 cm^{-1} (Figure 7g). The latter signal most likely results from an amide proton hydrogen bonding to the ester carbonyl. The small frequency shift between non-hydrogen-bonded and hydrogen-bonded N–H signals reflects the relatively weak hydrogen bond accepting properties of the ester carbonyl.[21c,d] Importantly, no hydrogen-bonded signal is observed in the range 3330–3360 cm^{-1}, demonstrating that the six-membered-ring hydrogen bond does not contribute to the 3351-cm^{-1} signal in **29**. In summary, the 13-membered ring intramolecular hydrogen bonded conformer of **29** appears to predominate while the 11-membered ring intramolecular hydrogen-bonded conformer seems to be a minor contributor in solution. Amides composed of **2**, which cannot form a 13-membered ring intramolecular hydrogen bond (e.g. **30**) only adopt a partially hydrogen-bonded conformation. This observation verifies the instability of the 11-membered ring intramolecular hydrogen bond relative to the 13-membered ring intramolecular hydrogen-bonded conformation, which is nearly completely formed at room temperature (e.g. imide **35**).

An IR study on diamide **31** derived from amino acid **3** reveals no intramolecular hydrogen bonding in dichloromethane at room temperature, consistent with what was expected (Figure 7h).

VT-NMR Results. Variable-temperature ^{1}H NMR spectroscopy was also used to probe intramolecular hydrogen bonding in amides composed of residues **1**, **2**, and **3**. NMR spectroscopy is complimentary to IR spectroscopy for analyzing hydrogen bonding because the time scale of the NMR experiment is much slower when compared to the IR time scale, allowing averaged behavior to be probed. A previous NMR study on amides derived from residue **1** demonstrates that intramolecularly hydrogen-bonded N–H's resonate downfield at room temperature (≈7.0–9.0 ppm) and exhibit a relatively large temperature dependence of the

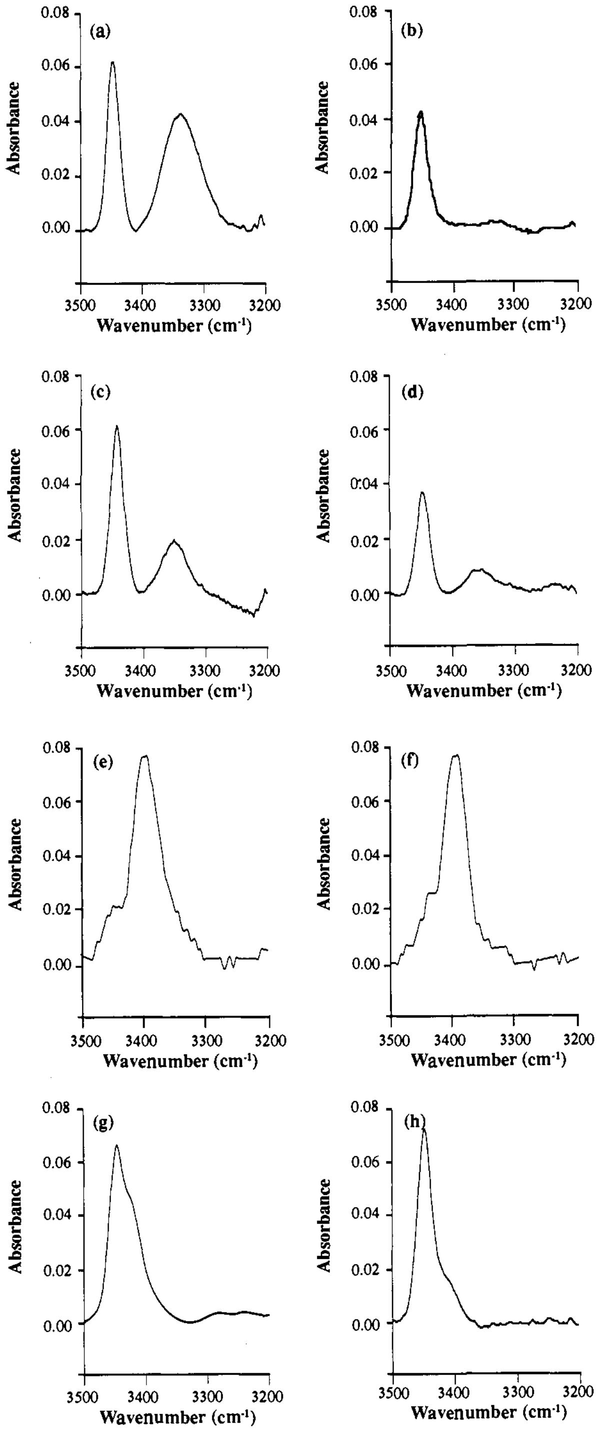

Figure 7. FT-IR spectral data from the N–H stretch region of 1.5 mM amide solutions in CH_2Cl_2 at room temperature after subtraction of the spectrum of pure CH_2Cl_2 and baseline correction. Data were collected on a Galaxy 6021 spectrometer. The sharp bands at 3440–3460 cm^{-1} are assigned to non-hydrogen-bonded N–H, and the broad bands at 3300–3360 cm^{-1} are assigned to an intramolecularly hydrogen-bonded N–H: (a) diamide **27** (maxima at 3336 and 3447 cm^{-1}); (b) diamide **28** (maximum at 3446 cm^{-1}); (c) diamide **29** (maxima at 3351 and 3443 cm^{-1}); (d) diamide **30** (maxima at 3360 and 3445 cm^{-1}); (e) imide **35** (maximun at 3396 cm^{-1} and a shoulder peak at 3444 cm^{-1}); (f) imide **36** (maximun at 3396 cm^{-1} and a shoulder peak at 3450 cm^{-1}); (g) amide **32** (maximum at 3445 cm^{-1} and a shoulder peak at 3424 cm^{-1} which is due to the weak hydrogen bonding between the amide proton and the ester carbonyl group); (h) diamide **31** (maximum at 3446 cm^{-1}).

chemical shift (−13 ppb/K) relative to free N–H's which resonate at ≈6.0 ppm at room temperature and exhibit a small temperature dependence of the chemical shift (−3 ppb/K).[8b] These chemical

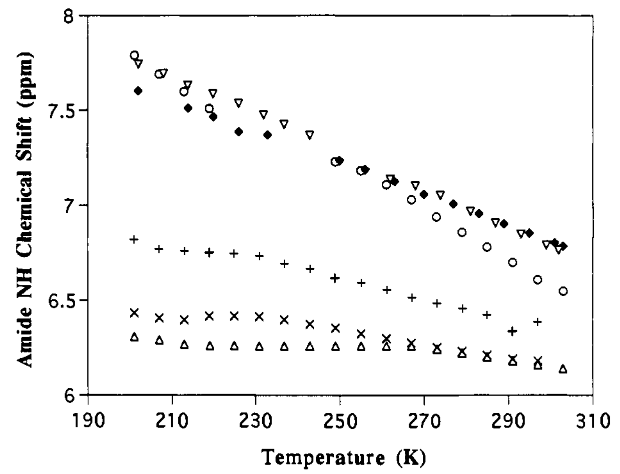

Figure 8. Temperature dependencies of the amide proton NMR chemical shifts for diamides **29** and **30**, imides **35** and **36**, and amide **32** in 1.5 mM CD_2Cl_2 solution. Data points around δ 7.4 and 7.6 ppm are missing due to overlap with the aromatic region of dibenzofuran. Chemical shifts are referenced to residual $CHDCl_2$ (5.320 ppm). Spectra were obtained on a Varian XL-400 spectrometer: (○, △) N–H's of **29**, (+) N–H of **30**, (×) N–H of **32**, (◆) N–H of **35**, and (▽) N–H of **36**.

shifts and temperature dependencies are consistent with what others have observed for amides in CH_2Cl_2.[21] The previously published NMR data on amides composed of **1** corroborates the conclusion from the infrared data that only the 15-membered ring intramolecularly hydrogen-bonded conformation is adopted.[8b]

Amide analogs of **2** were also studied by NMR (Figure 8). A proton NMR spectrum of amide **29** (1.5 mM in CD_2Cl_2 at room temperature) shows resonances for the amide protons at δ 6.16 and 6.61 ppm. The downfield signal shows a large temperature dependence ($\Delta\delta/\Delta T = -12$ ppb/K) consistent with an intramolecular hydrogen bond, whereas the upfield signal is not significantly influenced by temperature ($\Delta\delta/\Delta T = -1$ ppb/K) (Figure 8). Therefore, it can be inferred that one intramolecular hydrogen-bonding donor–acceptor pair (13-membered ring, as suggested by the IR studies) is preferred over the other pair in **29** (the 11-membered ring) (eq 2). Replacement of the isobutylamide group in **29** by a diethylamide functionality affords diamide **30**. The amide resonance in **30** exhibits an intermediate chemical shift and a moderate temperature dependence ($\Delta\delta/\Delta T = -5$ ppb/K), compatible with rapid equilibration between a non-hydrogen-bonded conformation and an 11-membered ring hydrogen-bonded conformation. This is consistent with the IR data which suggests that the 11-membered ring intramolecularly hydrogen-bonded conformer can only partially form in **30**. The 11-membered ring hydrogen bond is not nearly as stable as the 13-membered ring hydrogen-bond, which exhibits a significantly deshielded resonance and is more sensitive to temperature relative to the 11-membered ring hydrogen bond (Figure 8). A variable-temperature NMR study of the amide resonance in imide **35** (1.5 mM in CD_2Cl_2) reveals a significant temperature dependence of this resonance ($\Delta\delta/\Delta T = -8.1$ ppb/K) consistent with a 13-membered ring intramolecularly hydrogen-bonded conformation. That the imide N–H hydrogen bond in **35** exhibits a smaller temperature coefficient than the amide N–H hydrogen bond in **29** (−12 ppb/K) was expected since the imide carbonyl is not as good of a hydrogen bond acceptor as the amide carbonyl in **29**, as demonstrated by the FT-IR study on **35** discussed above. Nevertheless, the temperature dependencies of the amide proton in **35** and the downfield amide proton in **29** are very similar, strongly supporting the earlier proposal that the 13-membered ring conformer in **29** is the predominant conformer. Furthermore, the temperature dependences of the amide chemical shifts in imides **35** and **36** ($\Delta\delta/\Delta T = -8$ and −9 ppb/K, respectively) are nearly identical (Figure 8), demonstrating that the 13-membered ring hydrogen bond that predominates in **35** is comparable in

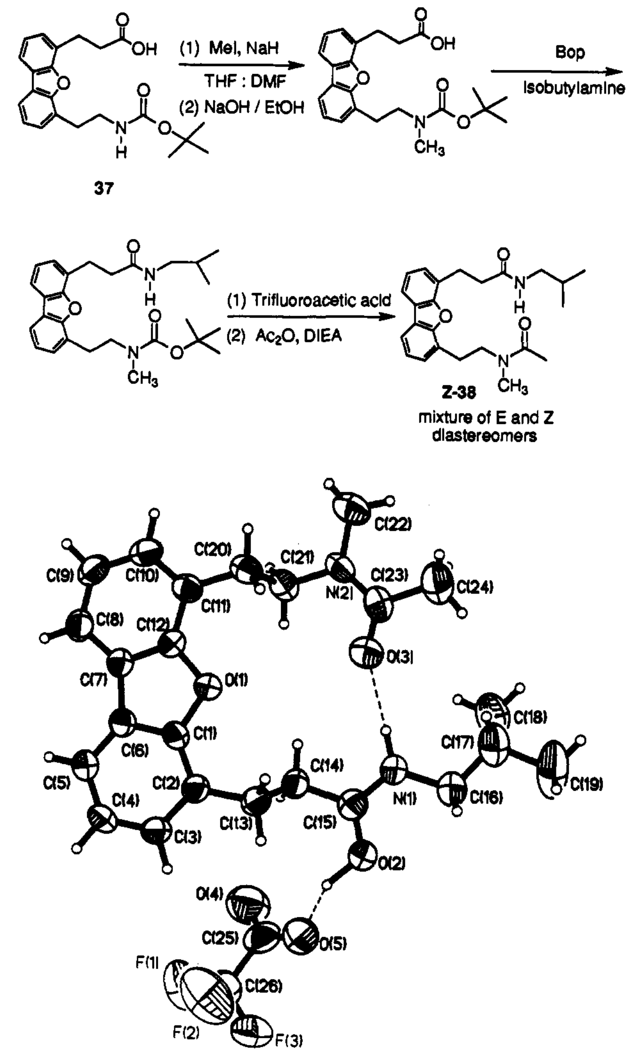

Figure 9. Outline of the preparation of **38** and an ORTEP depiction of the solid-state structure of the *Z* isomer of amide **38**. Note the 15-membered ring intramolecular hydrogen bond as well as the perpendicular relationship between the alkyl portion of **1** and the plane of the dibenzofuran ring. It is also interesting that **38** intramolecularly hydrogen bonds to trifluoroacetic acid and that the proton from TFA is closer to O2 than O5.

stability to the 15-membered ring intramolecular hydrogen bond that forms exclusively in amide and imide derivatives of **1** such as **27** and **36**, respectively. Replacement of the isobutylamide functionality in **29** with an ester affords analog **32**. Variable-temperature NMR analysis reveals a small temperature dependence of the amide resonance ($\Delta\delta/\Delta T = -3$ ppb/K) which is consistent with a non-, or very weakly, hydrogen-bonded amide. These spectral studies suggest that the possible six-membered intramolecular hydrogen bond in **29** cannot be responsible for the downfield resonance with a large temperature dependence observed in **29**.

An analogous ^{1}H NMR study was performed on diamide **31**. However, the temperature dependence of the chemical shift is not linear, indicating that the sample is possibly aggregating below 255 K. These studies were abandoned because the FT-IR spectroscopic data clearly indicate that amides composed of **3** are not intramolecularly hydrogen bonded.

Single Crystal X-ray Analysis. The synthesis of tertiary amide **38** is outlined in Figure 9. The *t*-Boc-protected amino acid **37** was treated with NaH and subsequently with MeI to afford an N-methylated analog of residue **1**. Hydrolysis of the methyl ester and conversion of the carboxyl group into an isobutyl amide group, followed by removal of the Boc protecting group and acetylation of the secondary amine, afford the tertiary amide **38**. After HPLC purification, crystals of (*Z*)-tertiary amide **38** were obtained from $CDCl_3$ by transferring a routine 5-mm NMR sample to a 500-mL round-bottomed flask which was capped with a septum to facilitate slow evaporation to afford rodlike crystals having the monoclinic space group $P2_1/n$ (14) over 12 h. The N to O distance determined by X-ray crystallography is 2.9 Å, consistent with a 15-membered-ring intramolecular hydrogen bond between the $\mathit{H}RNCH_2(CH_3)_2$ and the $\mathit{O}{=}C{-}CH_3$ as depicted in the ORTEP representation of the structure (Figure 9). This structure clearly shows that the aliphatic carbon–carbon bonds in the amino acid residue **1** are perpendicular to the plane of the aromatic ring. This conformation is that expected in nonpolar solvents and is slightly different from the conformation which is thought to be important for β-sheet nucleation in aqueous solution (*vide infra*) (Figure 1). The bond lengths, angles, and coordinates as well as isotropic and anisotropic displacement factors characterizing the solid state structure of **38** can be found in the supplementary material. VT-NMR and FT-IR data suggest that both the *E* and the *Z* isomers of **38** are intramolecularly hydrogen bonded in CH_2Cl_2 solution,[8b] consistent with the solid-state structure of the *Z* isomer.

Synthesis of Peptides. The NMR and FT-IR spectroscopic studies suggest that amide analogs of **1** are capable of adopting a 15-membered intramolecularly hydrogen-bonded conformation,[8b] which was confirmed by the X-ray crystallographic study of **38** and by the IR and NMR studies on imide **36**. Spectroscopic studies on amides and imides composed of **2** demonstrate that the 13-membered ring intramolecular hydrogen bond is preferred over the less stable 11-membered ring hydrogen-bonded conformation. Amides composed of **3** exhibit no tendency to form an intramolecular hydrogen bond. In order to examine whether the capability to form an intramolecular hydrogen bond has predictive value with regard to the nucleation of β-sheet structure in water, several related peptides were prepared. The propensity of the dibenzofuran-based amino acids **1**, **2**, and **3** to nucleate β-sheet formation in aqueous medium was examined with small acyclic heptapeptides whose sequences are based on the amphiphilic β-sheet portion of the cyclic monomeric peptide gramicidin S.[22] Conceptually, one of the two D-Phe-Pro dipeptide units (the $i + 1$ and $i + 2$ residues of the β-turn) in gramicidin S was excised and the other D-Phe-Pro dipeptide was replaced with a dibenzofuran-based amino acid, (i.e. **1**, **2**, or **3**) to afford the acyclic peptides shown in Figure 10.[8c,d] The Orn residues in gramicidin S were replaced with the structurally similar Lys residues because Lys is a common residue in proteins. Peptides **A-D** were synthesized on benzyhydrylamine resin by following the standard *t*-Boc synthesis protocols and employing the Bop reagent for carboxyl activation of the α-amino acids.[23] The β-turn mimic **1** was coupled to the growing peptide chain using the pentafluorophenyl active ester **9**, while amino acids **2** and **3** were coupled to the peptide chain using Bop activation of the *t*-Boc-protected amino acids **15** and **21**, respectively. The *t*-Boc-protected amino acids **15** and **21** were obtained by hydrolysis of carbamates **14** and **20**, respectively, and were used without further purification. Peptides **A-D** were deprotected and cleaved from the benzyhydrylamine resin employing high-HF[24] and purified by reverse-phase C_{18} HPLC. The primary structures of peptides **A-D** were

(22) (a) Ovchinnikov, Y. A.; Ivanov, V. T. *Tetrahedron* **1975**, *31*, 2177. (b) Ohnishi, M.; Urry, D. W. *Biochem. Biophys. Res. Commun.* **1969**, *36*, 194. (c) Ruttenberg, M. A.; King, T.; Craig, L. C. *Biochemistry* **1966**, *5*, 2857.

(23) Barany, G.; Merrifield, R. B. In *The Peptides*; Gross E., Meienhofer, J., Eds.; Academic Press: New York, 1980; Vol. 2, pp 3–254.

(24) Tam, J. P.; Merrifield, R. B. In *The Peptides; Analysis, Synthesis and Biology*; Udenfriend, S., Meienhofer, J., Eds.; Academic Press: New York, 1987; pp 185–244.

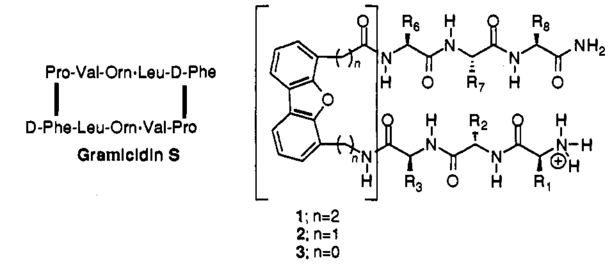

PEPTIDE	R1	R2	R3	R4	R5	R6	R7	R8
Peptide A	Val	Lys	Leu	1		Val	Lys	Leu-NH2
Peptide B	Val	Lys	Leu	2		Val	Lys	Leu-NH2
Peptide C	Val	Lys	Leu	3		Val	Lys	Leu-NH2
Peptide D	Val	Lys	Leu	D-Phe	Pro	Val	Lys	Leu-NH2

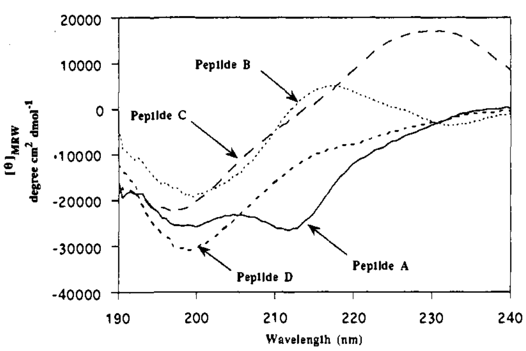

Figure 10. Far-UV CD spectra of peptides **A-D**. The CD data were collected on a Jasco J-600 spectropolarimeter at 25 °C using a 1-mm quartz cell. The sample concentration was 0.2 mM in 10 mM acetate buffer at pH 4.9. All spectra were corrected for buffer contributions and are reported in units of mean residue ellipticity.[29]

confirmed by amino acid analysis as well as by nominal resolution matrix assisted laser desorption mass spectroscopy.[25]

Circular Dichroism Studies. The CD spectrum of peptide A, containing **1**, exhibits two minima at 197 and 213 nm (Figure 10), which are assignable to random coil and β-sheet contributions, respectively.[8d] Peptide A adopts a monomeric β-sheet structure as discussed below.[8d] In addition, we have previously reported a two-dimensional (2D) NMR study on peptide A which supports a dynamic β-sheet conformation in aqueous solution.[8d] The CD spectra of peptides **B** and **C**, which incorporate amino acids **2** and **3** in the turn region, demonstrate that both of these peptides are unordered (Figure 10). The unnatural amino acid residues **2** and **3** are not functional as β-sheet nucleators in the acyclic gramicidin S sequence over the pH range 3–8, where peptide A is a dynamic monomeric β-sheet (Figure 10). The linear gramicidin S analog, peptide **D**, containing the natural Leu-D-Phe-Pro-Val reverse turn found in gramicidin S, was synthesized as a control to demonstrate that the acyclic gramicidin S sequence was not capable of adopting a folded β-sheet structure in aqueous solution. The pH-dependent far-UV CD spectra of peptide **D** demonstrates that it adopts a random coil conformation, indicating that the natural β-turn, as found in the cyclic peptide, is not sufficient to nucleate and stabilize a β-sheet secondary structure in an acyclic peptide in aqueous solution.

The near-UV CD spectra of peptides **A**, **B**, and **C** were recorded to probe the possible importance of the interaction of the dibenzofuran skeleton with the hydrophobic side chains of the flanking amino acid residues. Only peptide **A** exhibits a near-

(25) Chait, B. T.; Kent, S. B. H. *Science* **1992**, *257*, 1885 and references therein.

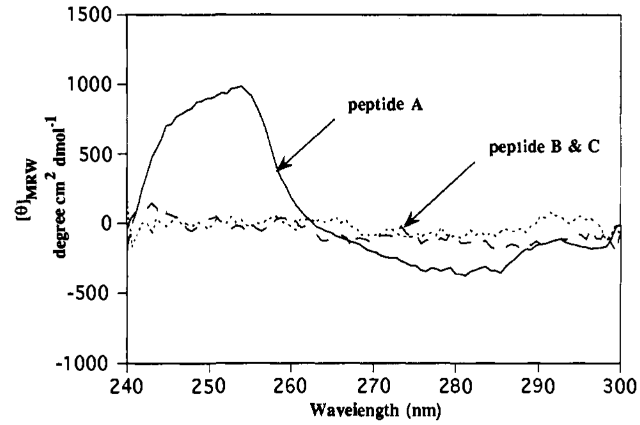

Figure 11. Near-UV CD spectra of peptides **A-C**. The CD data were collected on a Jasco J-600 spectropolarimeter at 25 °C using a 1-mm quartz cell. The sample concentration was 1.0 mM in 10 mM acetate buffer at pH 5.0. All spectra were corrected for buffer contributions and are reported in units of mean residue ellipticity.[29]

UV CD spectra resulting from the dibenzofuran chromophore (Figure 11), which indicates that the dibenzofuran skeleton in peptide A is in a rigid asymmetric hydrophobic environment. The presence of a near-UV CD signal supports the importance of the hydrophobic cluster in the folded state of peptide A, which has been verified by NOESY-NMR studies.[8d]

1D NMR Spectra of Peptides A, B, and C. The sequence specific assignments of the residues in peptide A as well as a discussion of the interpretation of the NOESY and COSY spectra have been communicated previously.[8d] Briefly, the methyl groups composing the Leu and Val residues flanking **1** are found to be shifted significantly upfield relative to the C-terminal Leu and N-terminal Val residues in peptide A, suggesting that the methyl groups are in the diamagnetic shielding cone of the dibenzofuran ring system. That the methyl groups were interacting with the face of the aromatic ring system was further supported by the NOE's observed between the methyl groups and the aryl protons of the dibenzofuran ring.[8d] Comparison of the aliphatic regions of the ^{1}H NMR spectra of peptides A-C reveals the absence of the upfield shifted Leu-3 and Val-6 methyls in peptides **B** and **C** (Figure 12), suggesting that the hydrophobic cluster does not form in peptides composed of residues **2** and **3**, respectively. The correlation between hydrophobic cluster formation and β-sheet nucleation argues in favor of the importance of this structural feature.[8c,d]

Characterization of Peptide A. Since peptide A adopts a partial β-sheet structure in aqueous solution, a detailed study of this peptide was undertaken in order to understand the basis for its structure. The CD spectra of peptide A as a function of pH are shown in Figure 13. The CD spectra for pH 3.0–7.5 are nearly identical, demonstrating that the structure of peptide A is pH independent over this range. This was expected since the charge state of the peptide is not being changed in this pH range. However, at pH's >7.5, the N-terminal positive charge is removed which reduces the solubility by enhancing intermolecular interactions of peptide A, resulting in an aggregated β-sheet structure. The structure of peptide A is also resistant to changes in ionic strength as discerned by CD. The spectra of peptide A do not change significantly in increasing NaCl concentrations up to 250 mM (data not shown). This is somewhat suprising since both increased electrostatic screening and the increased importance of the hydrophobic effect at elevated salt concentrations might have been expected to increase the amount of β-sheet structure relative to random coil structure. However, peptide A adopts a hydrophobic cluster conformation/partial β-sheet structure even under low-salt conditions and it may be that the structured part of the molecule remains unchanged, even at higher salt concentrations.[8c,d] The N- and C-terminal residues are disordered

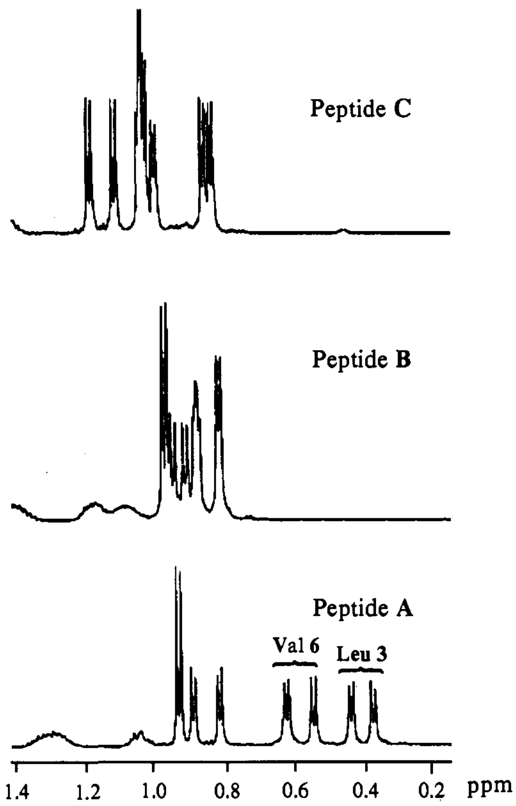

Figure 12. 1D NMR spectra of the Leu and Val aliphatic side chain regions of peptides **A-C** in deuterated acetate buffered 90% H_2O:10% D_2O at 25 °C. Note the significant upfield shift of the Leu-3 and Val-6 methyl groups in peptide **A** relative to those in peptides **B** and **C**. The upfield shift further supports the hydrophobic cluster conformation adopted by the Leu-3-**1**-Val-6 tripeptide unit in peptide **A**.

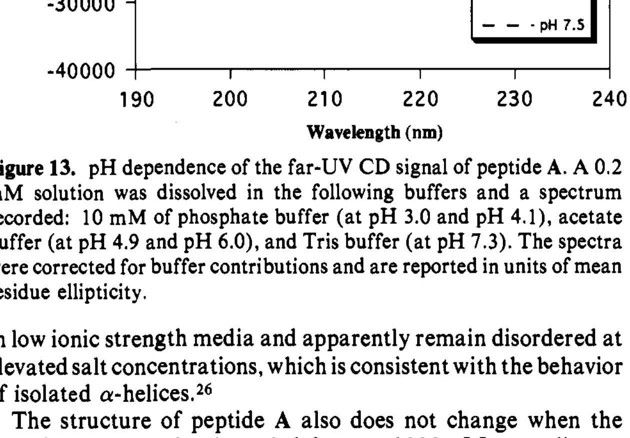

Figure 13. pH dependence of the far-UV CD signal of peptide **A**. A 0.2 mM solution was dissolved in the following buffers and a spectrum recorded: 10 mM of phosphate buffer (at pH 3.0 and pH 4.1), acetate buffer (at pH 4.9 and pH 6.0), and Tris buffer (at pH 7.3). The spectra were corrected for buffer contributions and are reported in units of mean residue ellipticity.

in low ionic strength media and apparently remain disordered at elevated salt concentrations, which is consistent with the behavior of isolated α-helices.[26]

The structure of peptide A also does not change when the peptide concentration is varied from 5–1000 μM according to far-UV CD analysis (data not shown). The concentration-independent CD spectra suggest that peptide A is monomeric in aqueous medium below pH 7.5. This interpretation was confirmed by the results obtained from equilibrium ultracentrifugation

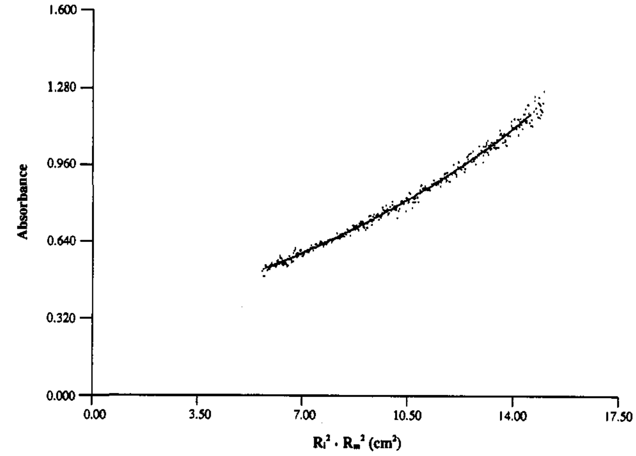

Figure 14. First pass analysis of the equilibrium ultracentrifugation data (50 000 rpm) plotted as absorbance versus the square of the radial position as measured from the sample meniscus. The curve fit to the data represents a single exponential fit to the sedimentation equilibrium equation $C_i r = C_i r_m e^{AM_i(r_i^2 - r_m^2)}$, which affords an apparent MW of 972 (monomer) at 23°C. A partial specific volume for the peptide of 0.84 cm^3/g and a solvent density of 0.998 g/cm^3 were used. The weight-averaged MW whether calculated across the boundary or at either end of the cell is nearly the same, ≈1000.

studies which yield a weight-averaged MW of 1000 for peptide A (Figure 14). It appears that the relatively high positive charge density of peptide A (three positive charges over seven residues) and the dynamic nature of the β-sheet structure help to prevent the peptide from undergoing self-association, which has historically proven to be a major problem in the *de novo* design of β-sheet structures.[4] It is known that the hydrophobic face of gramicidin S (composed of two Leu and two Val side chains) does not mediate face to face self-association.[27] Therefore, it may not be suprising that peptide A is monomeric in aqueous solution. However, peptide A is different from gramicidin S in that it also has the dibenzofuran skeleton interacting with the side chains of the flanking Leu and Val residues. Apparently, the increase in hydrophobic surface area of peptide A is compensated for by the disorder in the N- and C-terminal portions of peptide A's β-sheet, which prevents it from self-associating.

It is necessary to determine if it is possible for a small peptide such as peptide A to fold cooperatively, analogous to the behavior exhibited by proteins which are much larger.[1a] The denaturation of a polypeptide is usually probed spectroscopically as a function of denaturant concentration or temperature, affording a denaturation curve.[28] A sigmoidal denaturation curve indicates that the polypeptide of interest folds cooperatively. The linear thermal denaturation curve exhibited by peptide A obtained by monitoring the CD signal at 213 nm indicates that peptide A unfolds but does not do so cooperatively (data not shown) ($\Delta[\theta]_{MRW}/\Delta T = 107.5$ deg cm^2 $dmol^{-1}$ K^{-1}). Denaturation employing urea also generates a linear denaturation curve ($\Delta[\theta]_{MRW}/\Delta[\text{urea}] = 1221.5$ degree cm^2 $dmol^{-1}$ M^{-1}) (Figure 15). These results clearly demonstrate that peptide A is too small to fold cooperatively, which makes it impossible to measure the thermodynamic stability of peptide A relative to its unfolded state.[28] Interestingly, tridecapeptides containing **1** do fold cooperatively.[8d]

Evidence for the Importance of the Hydrophobic Cluster in β-Sheet Nucleation. Our approach for the formation of β-sheet structure is based on the hypothesis that sheet folding can be nucleated by an intramolecularly hydrogen-bonded hydrophobic cluster mediated by **1**.[8c,d] The hydrophobic cluster appears to be

(26) (a) Dradley, E. K.; Thomason, J. F.; Cohen, F. E.; Kosen, P. A.; Kuntz, I. D. *J. Mol. Biol.* **1990**, *215*, 607. (b) Miick, S. M.; Todd, A. P.; Millhauser, G. L. *Biochemistry* **1991**, *30*, 9498.

(27) Ruttenberg, M. A.; King, T.; Craig, L. C. *Biochemistry* **1966**, *5*, 2857.

(28) Pace, C. N.; Shirley, B. A.; Thomson, J. A. In *Protein Structure; a practical approach*; Creighton, T. E., Ed.; IRL Press: New York, 1989; pp 311–330.

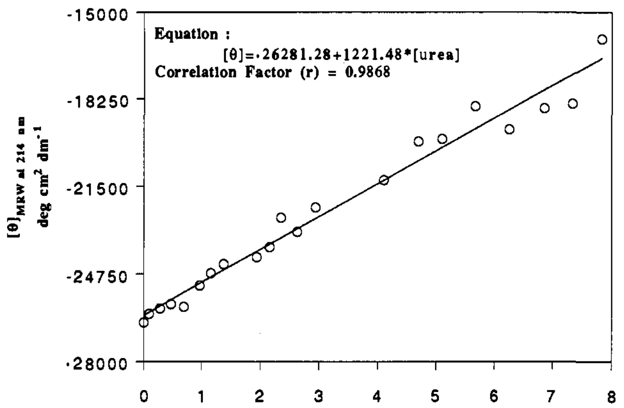

Figure 15. Dependence of the far-UV CD signal of peptide **A** at 214 nm on the urea concentration. A 0.23 mM solution of peptide **A** in 10 mM acetate buffer at pH 4.0 was incubated at the indicated urea concentration for 24 h. The spectra were corrected for buffer contributions and are reported in units of mean residue ellipticity.

Table 1[a]

peptide	R_1	R_2	R_3	R_4 R_5	R_6	R_7	R_8
A	Val	Lys	Leu	**1**	Val	Lys	Leu-NH_2
E	Val	Leu	Lys	**1**	Lys	Val	Leu-NH_2
F	Lys	Val	Leu	**1**	Val	Leu	Lys-NH_2
G	Val	Lys	Leu	**1**	Ala	Lys	Leu-NH_2
H	Val	Lys	Ala	**1**	Ala	Lys	Leu-NH_2
I	Val	Lys	Leu	**1**	Leu	Lys	Leu-NH_2
J	Val	Lys	Leu	**1**	Phe	Lys	Leu-NH_2
K	Val	Lys	Phe	**1**	Phe	Lys	Leu-NH_2

[a] See Figure 10 for a line drawing guide to the structures of these peptides.

critical for β-sheet nucleation in peptide **A** as discerned from near-UV CD studies[29] as well as 1- and 2D NMR experiments described above. Several peptides related to peptide **A** and containing residue **1** were prepared to further probe the importance of the hydrophobic cluster as well as the α-amino acid sequence requirements for β-sheet nucleation (Table 1).

The importance of side chain hydrophobicity in β-sheet nucleation mediated by residue **1** was addressed by preparing analogs of peptide **A** which have sequence variability in the positions flanking **1**. Peptide **E** has the same amino acid composition as peptide **A** but differs in that the residues 2 and 3, as well as 6 and 7, have been switched so that Lys residues now flank residue **1** (Table 1). Peptide **E** is incapable of adopting a β-sheet structure in aqueous solution as discerned from its far-UV CD spectrum (Figure 16). Apparently, this peptide is incapable of folding because a hydrophobic cluster does not form. The absence of a hydrophobic cluster in peptide **E** is verified by the absence of a near-UV CD spectrum (Figure 17). The sequence of peptide **E** does not allow for the formation of an amphiphilic β-sheet, such as that found in peptide **A**.[30] There was concern that its nonamphiphilic structure also may be, in part, responsible for peptide **E**'s inability to adopt a β-sheet structure. Therefore, peptide **F** was prepared, which cannot form an amphiphilic β-sheet structure, to probe the importance of amphiphilicity in the nucleation and stabilization of monomeric β-sheets. Peptide **F** can form a hydrophobic cluster as evidenced by its near-UV CD spectrum (Figure 17). The far-UV CD spectrum of peptide **F** demonstrates that it can adopt a β-sheet structure in aqueous solution (Figure 16). These results suggest that the amphiphilicity of the resulting sequence is relatively unimportant when compared to its ability to form a hydrophobic cluster. However, the relative amount of β-sheet structure in peptide **F** is less than in the case

(29) Schmid, F. X. In *Protein Structure; a practical approach*; Creighton, T. E., Ed.; IRL Press: New York, 1989; pp 251–285.
(30) Kaiser, E. T.; Kezdy, F. J. *Science* **1984**, *223*, 249.

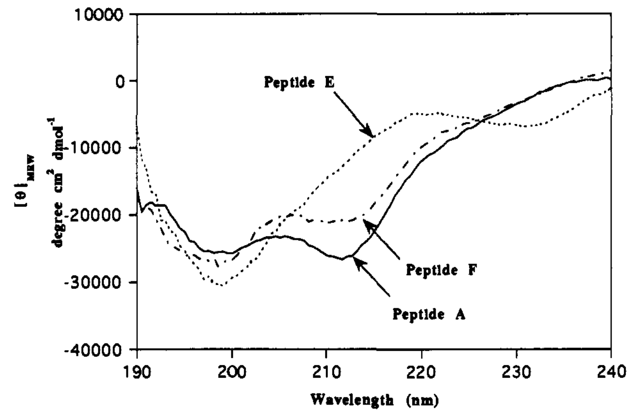

Figure 16. Far-UV CD spectra of 0.2 mM solutions of peptides **A**, **E**, and **F** in 10 mM acetate buffer at pH 4.9. The spectra were corrected for buffer contributions and are reported in units of mean residue ellipticity.

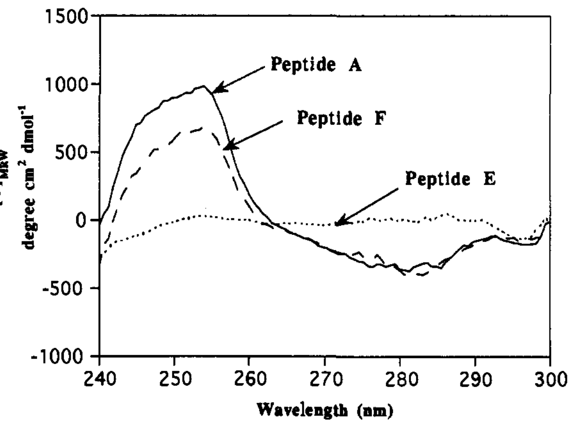

Figure 17. Near-UV CD spectra of 1.0 mM solutions of peptides **A**, **E**, and **F** in 10 mM acetate buffer at pH 4.0. All spectra were corrected for buffer contributions and are reported in units of mean residue ellipticity.

of peptide **A**, implying that the amphiphilicity of the resulting structure may play a minor role in stabilizing a monomeric antiparallel β-sheet structure by allowing the hydrophobic residues of the sheet to cluster.[30] A comparison of peptides **A** and **E** using CPK models reveals that the aliphatic portion of the Lys side chain is not bulky enough to bury a significant hydrophobic surface against the dibenzofuran ring system in peptide **E**. This most likely explains why hydrophobic cluster formation is not observed in peptide **E**.

Effects of Amino Acid Side Chain Hydrophobicity on Folding of Peptides. Peptides **G** and **H** were prepared to further probe the sequence requirements for hydrophobic cluster formation. The hydrophobic cluster conformation is presumably stabilized by the hydrophobic effect, and therefore, it is important that relatively large hydrophobic surfaces interact so that the thermodynamic advantage realized by dehydration of the interacting surfaces is significant. It is also important that the interacting hydrophobic surfaces have shape complimentarity so that voids or solvent molecules do not interfere with cluster formation. These ideas were tested with peptides **G** and **H** where one or both of the bulky hydrophobic flanking residues in peptide **A** were replaced with an Ala residue(s). Alanine has a methyl side chain which is significantly smaller than the isopropyl and isobutyl side chains of Val and Leu, respectively. As expected, the incorporation of Ala has deleterious effects on β-sheet formation in aqueous solution. Once one Ala is incorporated in place of Val-6 (peptide **G**), the amount of β-sheet structure decreases at the expense of random coil (Figure 18) because the hydrophobic cluster is not as well organized in this peptide for the reasons stated above. This interpretation is supported by the near-UV CD spectra of peptide **G**, which exhibits a spectrum

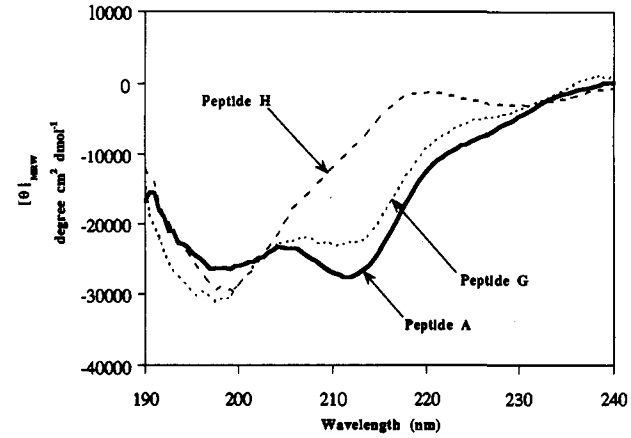

Figure 18. Far-UV CD spectra of 0.1 mM solutions of peptides **A**, **G**, and **H** in 10 mM acetate buffer at pH 4.0. All spectra were corrected for buffer contributions and are reported in units of mean residue ellipticity.

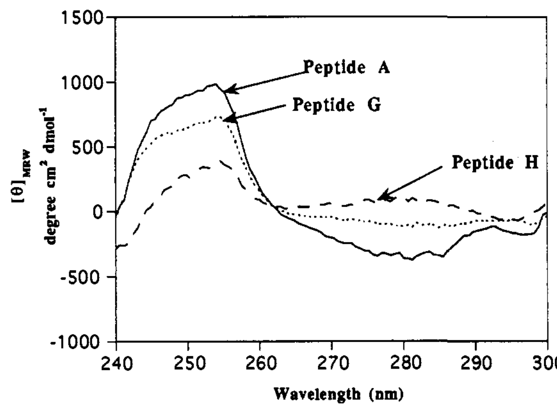

Figure 19. Near-UV CD spectra of 1.0 mM solutions of peptides **A**, **G**, and **H** in 10 mM acetate buffer at pH 4.0. All spectra were corrected for buffer contributions and are reported in units of mean residue ellipticity.

analogous to that of peptide **A** but having only two-thirds the intensity (Figure 19). Replacement of both Leu-3 and Val-6 in peptide **A** with Ala affords peptide **H**, which is incapable of β-sheet formation (Figure 18) because hydrophobic cluster formation is not favored. The instability of the hydrophobic cluster in peptide H is confirmed by the very weak near-UV CD spectrum exhibited by this peptide (Figure 19). Peptide I was prepared to further demonstrate the general requirement for hydrophobic α-amino acid residues in the positions flanking **1**. Replacement of the Val-6 residue in peptide **A** by a hydrophobic Leu residue affords peptide I, which adopts a β-sheet structure which is indistinguishable from that of peptide **A** by far-UV CD (data not shown). Furthermore, the analogous near-UV CD spectrum exhibited by peptide I suggests that the exact residues flanking **1** are not so important as long as they are hydrophobic in nature.

Effects of Interaction of Aromatic Ring Systems on Nucleation and Folding. π-Stacking, edge to face and randomly oriented aromatic–aromatic interactions have been shown to be important in stabilizing the hydrophobic core of proteins.[31] We rationalized that these same interactions may also prove to be useful for the nucleation of β-sheet structure via the formation of an aromatic hydrophobic cluster. This is made possible when **1** is flanked by an aromatic amino acid residue(s). Peptides **J** and **K** were synthesized where either one or both of the flanking residues in peptide **A** were replaced by Phe (Table 1). The far-UV CD spectrum of peptide **J**, which has a Phe for Val-6 replacement, is very encouraging in that the β-sheet minimum at 214 nm has increased relative to the random coil signal at 197 nm when compared to that of peptide **A** (Figure 20). That the hydrophobic cluster in peptide **J** is well organized is verified by the near-UV CD spectrum which is virtually identical to that of peptide **A** (data not shown). Replacement of both of the flanking residues in peptide **A** by Phe affords peptide **K**. The far-UV CD maximum at 197 nm and minimum at 210 nm suggest a β-sheet structure for peptide **K** (Figure 20).[32] The reduced mean residue ellipticity suggests that there may be a significant aromatic contribution to the far-UV CD spectrum. These contributions are usually positive and may explain the diminution in the band intensity at 210 nm.[32] Peptide **K** exhibits a very broad positive near-UV CD spectrum from 240 to 300 nm which supports, but does not establish unequivocally, a positive aromatic contribution to the far-UV CD spectrum. Future NMR experiments to further characterize the structure of peptide **K** will clarify its structure. The studies described here clearly demonstrate that aromatic–aromatic interactions can be employed to form a hydrophobic cluster which is capable of nucleating β-sheet structure. Recent studies to be published elsewhere also demonstrate that a charged His can be used in the flanking position to stabilize a nucleating conformation.

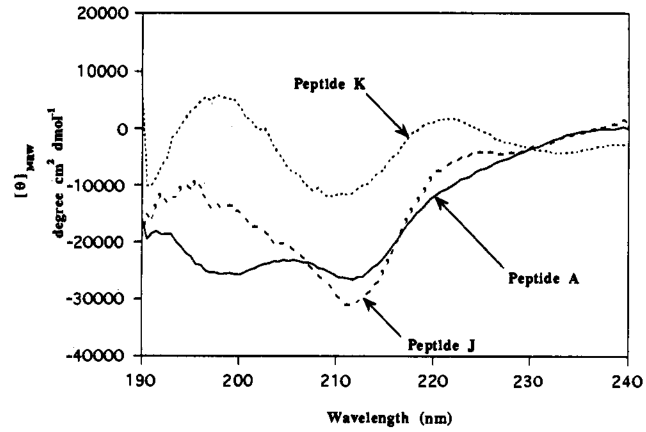

Figure 20. Far-UV CD spectra of 0.1 mM solutions of peptides **A**, **J**, and **K** in 10 mM acetate buffer at pH 4.9. All spectra were corrected for buffer contributions and are reported in units of mean residue ellipticity.

Discussion

The incorporation of an unnatural amino acid into an otherwise α-amino acid sequence in order to direct the folding of that sequence into a well-defined secondary or supersecondary structure should prove to be very useful in structural and functional bioorganic chemistry. Kemp and co-workers have been able to direct the folding of both α-helices and β-sheets by the incorporation of unnatural amino acids into α-amino acid sequences.[11b,33] The epindolidione nucleator employed by the MIT group mimics a β-strand and serves to nucleate β-sheet formation through hydrogen bonding. The dibenzofuran-based nucleator **1** is complimentary in that it replaces the $i + 1$ and $i + 2$ residues of a β-turn and serves to nucleate an antiparallel β-sheet structure, which should not be significantly perturbed by the nucleator itself. Residue **1** employs both hydrogen bonding and the hydrophobic effect, via the hydrophobic cluster, to nucleate antiparallel β-sheet formation. The major focus of the experimental work within is to understand the basis of **1**'s nucleating efficacy so as to be able to improve on the initial design and best utilize residue **1**.[8]

Spectroscopic and computational studies on amide analogs of residue **1** suggest that they can adopt two low-energy conformations with respect to residue **1** (Figure 1).[8b] The conformation adopted by **1** in the solid state (Figures 1A and 9) is the lowest energy conformer according to computational modeling studies.

(31) (a) Blundel, T.; Singh, J.; Burley, S. K.; Petsko, G. A. *Science* **1986**, *234*, 1005. (b) Burley, S. K.; Petsko, G. A. *Science* **1985**, *229*, 23. (c) Hunter, C. A.; Sanders, J. K. M. *J. Am. Chem. Soc.* **1990**, *112*, 5525.

(32) Perczel, A.; Park, K.; Fasman, G. D. *Proteins* **1992**, *13*, 57.

(33) Kemp, D. S.; Boyd, J. G.; Muendel, C. C. *Nature* **1991**, *352*, 451.

The solid-state conformation also appears to be the same conformation adopted in nonpolar solvents such as CH_2Cl_2. An alternative conformation is adopted by peptides composed of **1** in aqueous solution when the amino acid residues flanking **1** bear relatively large hydrophobic side chains. The hydrophobic effect apparently stabilizes an interaction between the dibenzofuran ring and the hydrophobic side chains of the flanking α-amino acid residues, affording the hydrophobic cluster conformation shown in Figure 1B-D. This conformation is sampled frequently during a dynamics run of simple amides such as **27** and is only slightly higher in energy than the solid-state conformer in a low dielectric medium such as CH_2Cl_2.[8b] The perpendicular orientation of the aminoethyl and the carboxyethyl groups with respect to the aromatic ring system is maintained in the hydrophobic cluster conformation of **1** as is the intramolecular 15-membered ring hydrogen bond (Figure 1B). The previously published NMR-based conformation of **1** in peptide A clearly demonstrates the presence of the hydrophobic cluster conformation in aqueous buffers.[8d]

A comparative study between amino acid residues **1**, **2**, and **3** reveals that amino acid **1** can form both a hydrophobic cluster and a 15-membered ring intramolecular hydrogen bond, which together appear sufficient to nucleate β-sheet formation. Residue **2** forms preferentially a 13-membered intramolecular hydrogen bond (eq 2, **29a**) but cannot form a hydrophobic cluster. Since this amino acid is incapable of nucleating sheet structure, it may be that hydrogen bonding is necessary, but not sufficient, to nucleate β-sheet formation in aqueous buffers. Residue **3** is incapable of forming either an intramolecular hydrogen bond or a hydrophobic cluster, and it is not suprising that this residue is ineffective as a β-sheet nucleator. The efficacy of residue **1** as a β-sheet nucleator appears to result from the intramolecularly hydrogen-bonded hydrophobic cluster conformation, which serves as a partial β-sheet template enabling neighboring residues to be added to the growing sheet with a favorable equilibrium constant.

Circular dichroism studies on analogs of peptide A, where α-amino acid substitutions have been made at one or both of the positions flanking residue **1**, demonstrate that the residue choice at these positions determines whether **1** is effective as a β-sheet nucleator. It appears that residue **1** must be flanked by hydrophobic amino acid residues in order for **1** to function as a β-sheet nucleator. The hydrophobic side chains of the flanking residues interact with the dibenzofuran skeleton to stabilize a hydrogen bonded hydrophobic cluster conformation. The cluster formed through the interaction of **1** with the hydrophobic side chains of the flanking α-amino acids appears to be responsible for the nucleation of antiparallel β-sheet formation in aqueous solution.

Conclusion

The dibenzofuran-based amino acids **1**, **2**, and **3** have been prepared and derivatized to afford simple amides which were studied by FT-IR and NMR, and in one case by X-ray crystallography. These studies reveal that 4-(2-aminoethyl)-6-dibenzofuranpropanonic acid (**1**) is capable of adopting a 15-membered ring intramolecularly hydrogen-bonded conformation of the type that will support antiparallel β-sheet structure. In addition, NMR and circular dichroism studies on peptides containing **1** reveal that this residue adopts a perpendicular conformation in which the face of the dibenzofuran ring system interacts with the side chains of the flanking hydrophobic amino acid residues in order to stabilize a hydrophobic cluster, which appears to be critical for the nucleation of β-sheet structure in aqueous solution. Neither residue **2** nor residue **3** nucleates β-sheet structure presumably because they are not able to form a hydrophobic cluster as discerned by near-UV CD and NMR studies. Residue **1** appears to be generally useful for the nucleation of β-sheet structure provided that it is flanked by hydrophobic α-amino acid residues.

Experimental Section

General Methods and Material for Synthesis of *t*-Boc-Protected 1, 2, and 3. The dibenzofuran used in these studies was purchased from Aldrich or from Lancaster. All organolithium reagents obtained from Aldrich were titrated prior to use. Dioxane, tetrahydrofuran (THF), and diethyl ether were distilled from sodium/benzophenone ketyl. *N,N,N',N'*-Tetramethylethylene diamine (TMEDA) was purchased from Aldrich and distilled from calcium hydride. Anhydrous *N,N*-dimethylformamide (DMF) was also obtained from Aldrich. Triethylamine (TEA) and diisopropylethylamine (DIEA) were refluxed over ninhydrin, distilled, and distilled again from calicum hydride. Ethyl acrylate (Eastman Kodak), pentafluorophenol (PCR Fluoroorganics), palladium acetate (Aldrich), tri-*o*-tolylphosphine (Strem), and other reagents were used without further purification. Flash chromatography was performed as described by Still.[34] Melting points were determined using a mel-temp apparatus and are uncorrected. Routine NMR spectra were recorded on a Varian XL-200E. Variable-temperature NMR experiments were performed on a Varian XL-400 spectrometer. FT-IR data were collected on a Galaxy 6021 spectrometer using a CaF_2 solution cell having a 3-mm pathlength. Mass determinations were carried out on a VG-70S double focusing high-resolution mass spectrometer. A matrix assisted laser desorption ionization (MALDI) mass spectrometer constructed by Dave Russell and co-workers was used to obtain nominal masses of peptides prepared within to corroborate their structure. Aqueous 1D NMR spectra were recorded on a Varian 500 Unity Plus spectrometer in deuterated acetate buffered 90% H_2O:10% D_2O at 25 °C. Far- and near-UV CD spectra were recorded on a Jasco J-600 spectrometer using a scan speed of 50 nm/min, a time constant of 0.5 s, a band width of 1 nm and are reported in mean residue ellipticity.[29] The data from the Jasco spectrometer was imported into the Macintosh version of KaleidaGraph and processed. Preparative HPLC was carried out on a dual pump system equipped with Altex 110A pumps and a 420 gradient programmer. The column employed was a Waters RCM Delta Pak C_{18} (15 μm, 300 Å, 25 × 100 mm) attached to a Knauer 86 variable-wavelength detector set at 254 nm. Solvent A was composed of 95% water, 5% acetonitrile (Fisher, Optima grade), and 0.2% TFA. Solvent B was composed of 5% water, 95% acetonitrile, and 0.2% TFA.

Metalation of Dibenzofuran and the Subsequent Reaction with I_2 Affords 4. A dry 3-L round-bottomed flask equipped with an overhead stirrer was charged with 43.7 g (260 mmol) of dibenzofuran. The flask containing the solid was flushed thoroughly with nitrogen, and 1 L of commercial anhydrous ether was added by cannulation. The solution was cooled to −78 °C using a dry ice/ethanol bath and 117.7 mL (780 mmol) of TMEDA was added via syringe. Then 600 mL (780 mmol) of *s*-BuLi (1.3 M in cyclohexane) was slowly added via an addition funnel. After the addition was complete, the mixture was allowed to warm to room temperature and was stirred for 24 h. In a separate 5-L round-bottomed flask equipped with an overhead stirrer and addition funnel, 304 g (1.2 mmol) of iodine in 1 L of dry ether was cooled to −78 °C. The suspension of 4,6-bis-lithiated dibenzofuran was transferred to the addition funnel using Teflon tubing (3-mm i.d.) and slowly added to the iodine solution. After the addition was complete, the mixture was allowed to slowly warm to room temperature and was stirred for an additional 12 h. The reaction mixture was then cooled to 0 °C, and 400 g of $NaHSO_3$ in 500 mL of water was added slowly while the mixture was stirred vigorously. The resulting slurry was stirred for an additional 15 min at room temperature. The ether layer was isolated by filtration and concentrated to afford 31 g of crude product. The residue from filtration was then extracted with hot $CHCl_3$ (4 × 300 mL), washed with water (3 × 200 mL), dried over anhydrous $MgSO_4$, and concentrated to afford another 60.2 g of crude product. The crude products were then combined and recrystallized using a mixture of chloroform/hexanes (8:5) to afford 90.6 g (83% yield) of pure diiodide **4**: mp 160–162 °C (lit. 160–161 °C);[16] ^1H NMR (acetone-d_6) δ 8.13 (dd, J = 7.7 Hz, J = 1.1 Hz, 2 H, Ar-1,9 *H*), 7.95 (dd, J = 7.8 Hz, J = 1.1 Hz, 2 H, Ar-3,7 *H*), 7.25 (t, J = 7.7 Hz, 2 H, Ar-2,8 *H*); ^{13}C NMR ($CDCl_3$) δ 155.88, 136.50, 124.72, 120.96, 75.60. Anal. Calcd for $C_{12}H_6I_2O$: C, 34.32; H, 1.44. Found: C, 34.46; H, 1.41.

Heck Cross-Coupling Reaction between Ethyl Acrylate and 4 Affords 5. A dry 250-mL round-bottomed flask fitted with a reflux condenser was charged with 50.0 g (119.1 mmol) of 4,6-diiododibenzofuran, 4.36

(34) Still, W. C.; Kahn, M.; Maitra, A. *J. Org. Chem.* **1978**, *43*, 2923.

g of tri-*o*-tolylphosphine, and 0.525 g (2.33 mmol) of palladium(II) acetate, and the flask and contents were purged with dry argon. Ethyl acrylate, 30 g (296.9 mmol), 30.2 g (298.2 mmol) of triethylamine, and 100 mL of DMF were then added to the flask. The mixture was placed in an oil bath at 95 °C for 0.5 h. The completion of the reaction was indicated by the formation of a black precipitate which was removed by filtration. After cooling to room temperature, the filtrate was diluted with 1 L of water, which precipitated the product. The crude product was then isolated by filtration and recrystallized from a mixture of ethanol/chloroform (9:1) to afford 40.3 g of **5** as a pale yellow solid (93% total yield): mp 143–144 °C; ^{1}H NMR (acetone-d_6) δ 8.19 (dd, *J* = 7.7 Hz, *J* = 1.24 Hz, 2 H, Ar-1,9 *H*), 8.01 (d, *J* = 16.3 Hz, 2 H, vinylic protons), 7.84 (dm, *J* = 7.6 Hz, 2 H, Ar-3,7 *H*), 7.49 (t, *J* = 7.6 Hz, 2 H, Ar-2,8 *H*), 7.01 (d, *J* = 16.2 Hz, 2 H, vinylic protons), 4.30 (q, *J* = 7.1 Hz, 2 H, OCH_2), 1.37 (t, *J* = 7.1 Hz, 3 H, CH_2CH_3); ^{13}C NMR ($CDCl_3$) δ 167.05, 154.10, 138.55, 128.28, 124.39, 123.53, 122.24, 121.68, 119.84, 60.62, 14.39. Anal. Calcd for $C_{22}H_{20}O_5$: C, 72.51; H, 5.53. Found: C, 72.50; H, 5.46.

Hydrolysis and Hydrogenation of 5 to Yield 6. A dry 500-mL round-bottomed flask was charged with 12 g (300 mmol) of sodium hydroxide, 300 mL of absolute ethanol, and 15 g (41.2 mmol) of diester **5**. The resulting suspension was heated at reflux for 2 h with vigorous stirring under a nitrogen atmosphere. The reaction mixture was cooled to room temperature and placed in an ice bath. The resulting solid was removed by vacuum filtration, washed with ethanol (3 × 20 mL), and dried under vacuum to afford a pale yellow solid. The crude carboxylate was transferred to a 500-mL hydrogenation bottle (Parr), dissolved in 250 mL of water, and mixed with 0.89 g of 10% palladium on activated carbon. The solution was agitated in a Parr apparatus under 50–55 psi of hydrogen at room temperature for 4 h.

The reaction mixture was then filtered through a 0.45-μm nylon membrane to remove the catalyst. The filtrate was cooled in an ice bath, and 12 M hydrochloric acid was slowly added with vigorous stirring until the pH reached 1–2 (pH paper). The resulting white precipitate was filtered, washed with water, and dried under vacuum to afford 12.0 g (93% yield) of diacid **6**. Analytical samples were obtained by recrystallization from ethanol: mp 204–206 °C; ^{1}H NMR (DMSO-d_6) δ 12.20 (s, O*H*), 7.95 (dd, *J* = 7.3 Hz, *J* = 1.6 Hz, 2 H, Ar-1,9 *H*), 7.37 (dd, *J* = 7.4 Hz, *J* = 1.6 Hz, 2 H, Ar-3,7 *H*), 7.29 (t, *J* = 7.4 Hz, 2 H, Ar-2,8 *H*), 3.19 (t, *J* = 7.7 Hz, 2 H, $ArCH_2CH_2$), 2.75 (t, *J* = 7.8 Hz, 2 H, $ArCH_2CH_2$); ^{13}C NMR (DMSO-d_6), δ 173.66, 153.62, 127.02, 124.51, 123.42, 122.96, 118.91, 33.26, 24.58. Anal. Calcd for $C_{18}H_{16}O_5$: C, 69.22; H, 5.16. Found: C, 68.97; H, 4.87.

Esterification of 6 to Afford the Monoester 7. A dry 100-mL round-bottomed flask equipped with a Soxhlet extractor containing powdered molecular sieves (3 Å) was charged with 4.6 g (14.7 mmol) of diacid **6** and 95 mL of anhydrous ethanol, and the mixture was stirred under reflux for 50 h. The reaction crude was concentrated and treated with 30 mL of hot chloroform. The chloroform solution was concentrated under reduced pressure, and the resulting solid was flash chromatographed on silica (hexanes/ethyl acetate/acetic acid 70:29:1) to afford 1.63 g (38% yield) of starting diacid **6**, 0.46 g (9% yield) of the diester, and 2.51 g (53% yield) of monoester **7**: mp 92–93 °C; ^{1}H NMR (acetone-d_6) δ 10.65 (bs, O*H*), 7.92 (dd, *J* = 7.4 Hz, *J* = 1.5 Hz, 2 H, Ar-1,9 *H*), 7.39 (m, 2 H, Ar-3,7 *H*), 7.30 (m, 2H, Ar-2,8 *H*), 4.07 (q, *J* = 7.1 Hz, 2 H, O-CH_2), 3.31 (t, *J* = 7.6 Hz, 4 H, 2CH_2), 2.85 (m, 4 H, 2CH_2), 1.16 (t, *J* = 7.1 Hz, 3 H, CH_3); ^{13}C NMR ($CDCl_3$) δ 178.91, 173.28, 154.38, 127.17, 127.12, 124.47, 124.30, 124.18, 122.89, 119.01, 118.90, 60.63, 34.28, 33.95, 25.48, 25.23, 14.19. Anal. Calcd for $C_{20}H_{20}O_5$: C, 70.58; H, 5.92. Found: C, 70.57; H, 5.90.

Schmidt Rearrangement of 7 Affords 8. A dry 50-mL round-bottomed flask was charged with 3.17 g (9.32 mmol) of monoester **7**, 28 mL of *tert*-butyl alcohol, 0.94 g (9.32 mmol) of triethylamine, and 3.08 g (11.2 mmol) of diphenylphosphonic azide. The homogeneous solution was heated at reflux for 24 h and cooled to room temperature. The solvent was removed under reduced pressure, and the resulting oil was dissolved in ether (40 mL). This solution was washed with 2 M citric acid (3 × 30 mL), 5% sodium bicarbonate (3 × 30 mL), and water (2 × 40 mL). The organic layer was dried (sodium sulfate) and concentrated to afford 4.11 g of a pale yellow solid. The crude was recrystallized from 40 mL of a 3:1 EtOH/water mixture to afford, upon cooling, (5 °C for several hours) 2.88 g (75 % yield) of carbamate **8**: mp 76–77 °C; ^{1}H NMR (acetone-d_6) δ 7.92 (dd, *J* = 7.4 Hz, *J* = 1.6 Hz, 2 H, Ar-1,9 *H*), 7.54 (m, 4 H, Ar-2,3,7,8 *H*), 6.15 (bs, 1 H, N-*H*), 4.08 (q, *J* = 7.12 Hz, 2 H, O-CH_2), 3.55 (q, *J* = 6.2 Hz, 2 H, $ArCH_2CH_2NH$), 3.31 (t, *J* = 7.9 Hz, 2 H, $ArCH_2CH_2$), 3.19 (t, *J* = 7.3 Hz, 2 H, $ArCH_2CH_2$), 2.85 (t, *J* = 7.8 Hz, 2 H, $ArCH_2CH_2$), 1.34 (s, 9 H, t-Bu), 1.17 (t, *J* = 7.1 Hz, 3 H, CH_3); ^{13}C NMR ($CDCl_3$) δ 172.90, 155.88, 154.62, 154.38, 127.74, 127.13, 124.48, 124.26, 124.19, 123.11, 122.94, 122.87, 118.97, 118.86, 79.14, 60.46, 40.48, 34.19, 30.58, 28.33, 25.35, 14.19. Anal. Calcd for $C_{24}H_{29}NO_5$: C, 70.05; H, 7.10. Found: C, 70.25; H, 7.14.

Hydrolysis of 8 to 37 and Subsequent Esterification Yields the Pentafluorophenyl Active Ester 9. A 50-mL round-bottomed flask charged with 4 g (9.7 mmol) of **8**, 30 mL of absolute ethanol, and 0.36 g (14.6 mmol) of NaOH was heated at reflux for 2 h. The solvent was removed under reduced pressure, affording a solid which was partitioned between 50 mL of CH_2Cl_2 and 100 mL of 0.5 M citric acid. The organic layer was separated, and the aqueous layer was washed with CH_2Cl_2 (2 × 50 mL). The organic layers were combined, dried ($MgSO_4$), and concentrated to afford 3.52 g (95% yield) of **37** as a pale yellow oil.

Crude **37** along with 1.8 g (10 mmol) of pentafluorophenol dissolved in 50 mL of ethyl acetate was cooled to 0 °C, and 2 g (9.5 mmol) of DCC was added in one portion. After 30 min, the ice bath was removed and the heterogeneous mixture was stirred for 14 h at room temperature. The reaction flask was cooled and the dicyclohexylurea was filtered off, which was removed under reduced pressure to afford 5.36 g of a pale yellow solid. This crude was recrystallized from 44 mL of hexanes/ethyl acetate (10:1) to afford 4.69 g (88% yield) of **9** as a white solid: mp 93–94 °C; ^{1}H NMR ($CDCl_3$) δ 7.84 (m, 2 H, Ar-1,9 *H*), 7.31 (m, 4 H, Ar-2,3,7,8 *H*), 4.69 (bs, 1 H, N*H*), 3.59 (q, *J* = 6.4 Hz, 2 H, $ArCH_2CH_2NH$), 3.46 (t, *J* = 7.3 Hz, 2 H, $ArCH_2CH_2$), 3.22 (m, 4 H, $ArCH_2CH_2$), 1.39 (s, 9 H, t-Bu); ^{13}C NMR ($CDCl_3$) δ 168.80, 155.87, 154.65, 154.25, 127.88, 127.10, 124.42, 124.18, 123.15, 123.10, 123.05, 119.39, 119.06, 79.17, 40.47, 33.21, 30.61, 28.31, 25.18. MS *m/z* (M^+) calcd 549.1575, obsd 549.1582.

Cu(I) Catalyzed Cross-Coupling between 4 and Diethyl Malonate Affords 10. A dry 250-mL round-bottomed flask was charged with 1.14 g (28.57 mmol) of NaH as a 60% dispersion in mineral oil. The mineral oil was removed by washing the NaH with anhydrous diethyl ether and removing the mineral oil–ether solution by syringe (2 × 3 mL). The remaining ether was evaporated with an argon stream. Anhydrous dioxane (60 mL) was then added via syringe and the suspension was cooled to 0 °C, followed by the addition of 4.61 g (28.61 mmol) of diethyl malonate in 20 mL of anhydrous dioxane by cannulation. After the transfer was complete, the reaction mixture was allowed to warm to room temperature and a mixture of 4.10 g (28.61 mmol) of copper(I) bromide and 4.00 g (9.53 mmol) of diiode **4** was added. The resulting suspension was heated at reflux for 2 h. After it was cooled to room temperature, the slurry was diluted with 100 mL of $CHCl_3$ and the suspended solid was removed by filtration. The organic layer was concentrated under reduced pressure to afford a green viscous oil which was purified by flash chromatography on silica (hexanes/ethyl acetate 8:2) to yield 3.08 g (72% yield) of **10**: mp 107–108 °C; ^{1}H NMR (200 MHz, $CDCl_3$) δ 7.90 (m, 2 H, Ar-3,9 *H*), 7.82 (dd, *J* = 8.0 Hz, *J* = 1.2 Hz, 1 H, Ar-1 *H*), 7.62 (dd, *J* = 7.7 Hz, *J*= 0.8 Hz, 1 H, Ar-7 *H*), 7.39 (t, *J* = 7.7 Hz, 1 H, Ar-8 *H*), 7.11 (t, *J* = 8.0 Hz, 1 H, Ar-2 *H*), 5.41 (s, 1 H, Ar-C*H*), 4.29 (q, *J* = 7.2 Hz, 4 H, –OCH_2CH_3), 1.30 (t, *J* = 7.2 Hz, 6 H, –OCH_2CH_3); ^{13}C NMR ($CDCl_3$) δ 168.26, 136.70, 128.45, 125.17, 125.12, 123.95, 121.55, 121.16, 118.16, 62.42, 51.96, 14.29; IR (KBr) 1743, 1734, 1190, 1172, 1163 cm^{-1}; MS *m/z* (M^+) calcd 452.0121, obsd 452.0098.

Hydrolysis and Decarboxylation of 10 Affords 11. A dry 100-mL round-bottomed flask was charged with 8.00 g (17.70 mmol) of **10**, 30 mL of ethanol, and 30 mL of a 1 N NaOH solution. The mixture was heated at reflux for 2 h, cooled to 0 °C, and acidified slowly by the addition of 10 mL of 12 M HCl at 0 °C. The solution was then heated at reflux for an additional 12 h. After cooling, the solution was diluted with 50 mL of water and basified with 5 N NaOH until the pH was >10. The insoluble residue was removed by filtration. Acidification of the filtrate with 12 M HCl afforded a white suspension which was filtered off and dried under reduced pressure to yield 6.17 g (99% yield) of **11**: mp 189–191 °C; ^{1}H NMR (200 MHz, DMSO-d_6) δ 12.52 (bs, 1H, COO*H*), 8.14 (dd, *J* = 7.7 Hz, *J* = 1.1 Hz, 1 H, Ar-3 *H*), 8.04 (dd, *J* = 7.4 Hz, *J* = 1.6 Hz, 1 H, Ar-9 *H*), 7.89 (dd, *J* = 7.7 Hz, *J* = 1.1 Hz, 1 H, Ar-1 *H*), 7.47 (dd, *J* = 7.4 Hz, *J* = 1.6 Hz, 1 H, Ar-7 *H*), 7.37 (t, *J* = 7.4 Hz, 1 H, Ar-8 *H*), 7.20 (t, *J* = 7.7 Hz, 1 H, Ar-2 *H*), 3.95 (s, 2 H, Ar-CH_2); ^{13}C NMR (DMSO-d_6) δ 171.50, 155.49, 153.56, 135.87, 129.31, 124.97, 124.12, 123.58, 123.37, 121.14, 120.32, 119.39, 76.38, 34.67; IR (KBr) 3459 (br), 1703 cm^{-1}; MS *m/z* (M^+) calcd 351.9596, obsd 351.9590.

Esterification of 11 Affords 12. A dry 250-mL round-bottomed flask was charged with 7.13 g (20.31 mmol) of iodoacid **11** and 200 mL of chloroform. The flask and contents were thoroughly flushed with argon, and 48.20 g (405 mmol) of thionyl chloride was added slowly. The resulting solution was heated at reflux for 3 h, after which the solvent and the excess thionyl chloride were removed under reduced pressure. The remaining light yellow solid was cooled to 0 °C, 80 mL of absolute ethanol was added slowly to the flask, and the mixture was heated at reflux for 30 min. The excess ethanol was removed under reduced pressure, and the remaining solid was purified by flash chromatography on silica (hexanes/ethyl acetate 4:1) to afford 7.56 g (98% yield) of iodoester **12**: mp 99–100 °C; ^{1}H NMR ($CDCl_3$) δ 7.85 (m, 3 H, Ar-1,3,9 *H*), 7.41 (dd, J = 7.4 Hz, J = 1.6 Hz, 1 H, Ar-7 *H*), 7.33 (t, J = 7.4 Hz, 1 H, Ar-8 *H*), 7.10 (t, J = 7.7 Hz, 1 H, Ar-2 *H*), 4.23 (q, J = 7.2 Hz, 2 H, $-OCH_2CH_3$), 4.04 (s, 2 H, $ArCH_2$), 1.29 (t, J = 7.2 Hz, 3 H, $-OCH_2CH_3$); ^{13}C NMR ($CDCl_3$) δ 170.80, 135.96, 128.66, 124.72, 124.43, 123.30, 120.64, 120.09, 118.81, 75.49, 61.12, 35.21, 14.31; IR (KBr) 1728, 1194, 1180 cm^{-1}; MS m/z (M^+) calcd 379.9909, obsd 379.9862.

Cyanation of 12 with CuCN Affords 13. A dry 250-mL round-bottomed flask was charged with 7.50 g (19.79 mmol) of iodoester **12**, 4.43 g (49.98 mmol) of copper(I) cyanide, and 100 mL of anhydrous DMF. After the flask and its contents were flushed with argon, the reaction mixture was heated at reflux for 2.5 h. After cooling, the reaction slurry was poured with stirring into 100 mL of dichloromethane and the suspended solid was removed by filtration. The filtrate was concentrated under reduced pressure to afford a green product which was purified by flash chromatography on silica (hexanes/ethyl acetate 7:3) to afford 5.47 g (99% yield) of **13** as a white solid: mp 114–116 °C; ^{1}H NMR ($CDCl_3$) δ 8.13 (dd, J = 7.8 Hz, J = 1.2 Hz, 1 H, Ar-3 *H*), 7.78 (m, 2 H, Ar-1,9 *H*), 7.41 (m, 3 H, Ar-2,7,8 *H*), 4.23 (q, J = 7.2 Hz, 2 H, $-OCH_2CH_3$), 4.03 (s, 2 H, $ArCH_2$), 1.30 (t, J = 7.2 Hz, 3 H, $-OCH_2CH_3$); ^{13}C NMR ($CDCl_3$) δ 170.57, 155.87, 154.87, 130.51, 129.70, 125.84, 125.55, 123.99, 123.08, 122.81, 119.96, 119.10, 114.99, 96.72, 61.26, 34.89, 14.22; IR (KBr) 2230, 1732, 1173, 1165 cm^{-1}; MS m/z (M^+) calcd 279.0895, obsd 279.0886.

Reduction of 13 Followed by *t*-Boc Protection Affords 14. Cyanoester **13**, 1.50 g (5.38 mmol), in 90 mL of ethanol (saturated with ammonia)[20] was hydrogenated over excess Raney nickel at room temperature for 2 days under a H_2 pressure of 50–55 psi by employing a Parr hydrogenator. The resulting solution was concentrated to give a pale green oil which was transferred to a 50-mL round-bottomed flask containing 1.76 g (8.07 mmol) of di-*tert*-butyl dicarbonate and 6 mL of anhydrous THF. The solution was then heated at reflux for 2 h, after which the solvent was removed under reduced pressure. The remaining solid was dissolved in 100 mL of $CHCl_3$ and washed with 2 M citric acid (3 × 10 mL), 5% sodium bicarbonate (3 × 10 mL), and water (3 × 15 mL). The organic layer was dried over anhydrous $MgSO_4$ and concentrated to afford a white solid which was purified by flash chromatography on silica (hexanes/ethyl acetate 7:3) to afford 1.85 g (90% yield) of pure carbamate **14**: mp 74–75 °C; ^{1}H NMR ($CDCl_3$) δ 7.84 (d, J = 7.2 Hz, 2 H, Ar-1,9 *H*), 7.35 (m, 4 H, Ar-2,3,7,8 *H*), 5.17 (bs, 1 H, N*H*), 4.69 (d, J = 5.9 Hz, 2 H, $ArCH_2NH$), 4.21 (q, J = 7.2 Hz, 2 H, $-OCH_2CH_3$), 4.00 (s, 2 H, $ArCH_2CO$), 1.47 (s, 9 H, *t*-Bu), 1.27 (t, J = 7.2 Hz, 3 H, $-OCH_2CH_3$); ^{13}C NMR ($CDCl_3$) δ 171.51, 156.51, 155.16, 128.70, 126.87, 124.88, 124.67, 123.53, 123.41, 120.37, 120.24, 118.92, 61.38, 39.85, 35.57, 20.56, 14.44; IR (KBr) 3364, 1738, 1684, 1532, 1285 cm^{-1}; MS m/z (M^+) calcd 383.1733, obsd 383.1714. Anal. Calcd for $C_{22}H_{25}O_5N$: C, 68.90; H, 6.58. Found: C, 68.87; H, 6.58.

Hydrolysis of 14 Affords 15. A 10-mL round-bottomed flask was charged with 0.50 g (1.31 mmol) of **14**, 0.06 g (1.50 mmol) of NaOH, and 5 mL of methanol, and the solution was heated at reflux for 2 h. After the solvent was removed under reduced pressure, the residue was dissolved in 25 mL of water and the solution was acidified using 8 mL of 2 M citric acid. The suspended solid was isolated by filtration and dried under vacuum to afford 0.46 g (99% crude yield) of crude carbamate acid **15**, which was employed in peptide synthesis and in the preparation of amide derivatives without further purification.

Dicyanation of Diiodide 4 Affords 16. A dry 50-mL round-bottomed flask was charged with 10.5 g (25 mmol) of diiodide **4** and 8.96 g (100 mmol) of copper(I) cyanide. After the flask and its contents were flushed with argon, 100 mL of anhydrous DMF was added and the resulting solution was heated at reflux for 2 h. The reaction mixture was cooled and poured with stirring into 100 mL of dichloromethane. The suspended solid was removed by filtration. The filtrate was then concentrated under reduced pressure to afford a yellowish green product **16**, 5.18 g (95% yield). White needle-shaped crystals were obtained by recrystallization from a mixture of chloroform/hexanes (8:1): mp 233–235 °C; ^{1}H NMR ($CDCl_3$) δ 8.23 (dd, J = 7.7 Hz, J = 1.3 Hz, 2 H, Ar-1,9 *H*), 7.85 (dd, J = 7.8 Hz, J = 1.3 Hz, 2 H, Ar-3,7 *H*), 7.54 (t, J = 7.7 Hz, 2 H, Ar-2,8 *H*); ^{13}C NMR ($CDCl_3$) δ 132.26, 127.43, 124.73, 123.84, 114.47, 95.87; IR (KBr) 2237, 1421, 1414, 1192 cm^{-1}; MS m/z (M^+) calcd 218.0480, obsd 218.0485.

Hydrolysis of 16 Affords 17. A dry 500-mL round-bottomed flask was charged with 7.2 g (33 mmol) of dinitrile **16**, 200 mL of methanol, and 200 mL of 1 N NaOH. The flask was flushed with argon, and the resulting mixture was heated at reflux for 24 h. After the mixture cooled to room temperature and insoluble impurities were removed by filtration, the filtrate was acidified with 2 M HCl to afford a white suspension. The suspended solid was filtered off and washed with water (3 × 30 mL), affording 8.37 g (99% yield) of white solid **17** after the sample was dried under vacuum. The purity was higher than 98% as determined by ^{1}H NMR. An analytical sample was obtained by recrystallization from a large amount of hot methanol (yellow crystals): mp 323–325 °C (lit. 325 °C);[37] ^{1}H NMR (DMSO-d_6) δ 8.13 (dd, J = 7.7 Hz, J = 1.3 Hz, 2 H, Ar-1,9 *H*), 8.09 (dd, J = 7.8 Hz, J = 1.3 Hz, 2 H, Ar-3,7 *H*), 7.57 (t, J = 7.7 Hz, 2 H, Ar-2,8 *H*); ^{13}C NMR (DMSO-d_6) δ 165.55, 154.50, 130.18, 162.02, 124.77, 123.53, 116.74; IR (KBr) 3397(br), 1655, 1417, 1188 cm^{-1}; MS m/z (M^+) calcd 256.0371, obsd 256.0371.

Esterification of 17 Affords 18. A dry 250-mL round-bottomed flask was charged with 5.00 g (19.53 mmol) of diacid **17** and 100 mL of chloroform. The reaction flask and its contents were flushed with argon, and 69.70 g (586 mmol) of thionyl chloride was then added slowly via syringe. The reaction mixture was heated at reflux for 3 h, after which the solvent and the excess thionyl chloride were removed under reduced pressure. The remaining light yellow solid was then cooled to 0 °C, 30 mL of absolute ethanol was added slowly into the flask, and the mixture was allowed to warm slowly to room temperature and then heated at reflux for 1 h. The excess ethanol was removed under reduced pressure, and the resulting pale yellow solid was flash chromatographed on silica (hexanes/ethyl acetate 4:1) to afford 5.91 g (97% yield) of pure diester **18**: mp 91–93 °C; ^{1}H NMR ($CDCl_3$) δ 8.16 (dd, J = 7.5 Hz, J = 1.4 Hz, 2H, Ar-1,9 *H*), 8.13 (dd, J = 7.5 Hz, J = 1.4 Hz, 2 H, Ar-3,7 *H*), 7.43 (t, J = 7.5 Hz, 2 H, Ar-2,8 *H*), 4.55 (q, J = 7.2 Hz, 4H, $-OCH_2CH_3$), 1.53 (t, J = 7.2 Hz, 6H, $-OCH_2CH_3$); ^{13}C NMR ($CDCl_3$) δ 164.61, 155.12, 129.92, 125.06, 124.87, 122.90, 116.23, 61.40, 14.40; MS m/z (M^+) calcd 312.0998, obsd 312.0985.

Limited Hydrolysis of 18 Affords Monoester 19. A dry 100-mL round-bottomed flask was charged with 3.0 g (9.62 mmol) of diester **18**, 0.38 g (9.62 mmol) of powdered sodium hydroxide, and 60 mL of anhydrous ethanol. The reaction mixture was then heated at reflux for 2 h. After the solvent was removed under reduced pressure, the remaining solid was dissolved in 50 mL of water and the solution was acidified by adding 20 mL of 1 M citric acid. The resulting slurry was extracted with dichloromethane (4 × 20 mL). The suspended solid was filtered off and washed with dichloromethane (2 × 10 mL) to afford 0.99 g (40% yield) of pure diacid **17**. The CH_2Cl_2 layers were combined and extracted with 1 M $KHCO_3$ (3 × 15 mL), washed with water (2 × 10 mL), dried (anhydrous $MgSO_4$), and concentrated to afford 0.59 g (20% yield) of the starting diester **18**. The $KHCO_3$ fractions were combined and acidified with 35 mL of 2 M citric acid. The resulting slurry was extracted with CH_2Cl_2 (3 × 20 mL). The organic layers were isolated, washed with water (2 × 10 mL), dried over anhydrous $MgSO_4$, and concentrated to afford 1.09 g (40% yield) of the monoacid monoester **19**: mp 192–193 °C; ^{1}H NMR (DMSO-d_6) δ 8.49 (m, 2 H, Ar-1,9 *H*), 8.09 (dd, J = 7.7 Hz, J = 1.2 Hz, 2 H, Ar-3,7 *H*), 7.57 (m, 2 H, Ar-2,8 *H*), 4.43 (q, J = 7.2 Hz, 2 H, $-OCH_2CH_3$), 2.51 (bs, 1 H, O*H*), 1.45 (t, J = 7.2 Hz, 3 H, $-OCH_2CH_3$); ^{13}C NMR (DMSO-d_6) δ 165.69, 164.38, 154.48, 151.97, 130.30, 129.86, 126.51, 126.17, 124.93, 124.71, 123.65, 116.77, 115.73, 61.20, 14.02; MS m/z (M^+) calcd 284.0685, obsd 284.0675.

Schmidt Rearrangement of 19 Affords 20. A dry 50-mL round-bottomed flask was charged with 3.00 g (10.56 mmol) of **19**, 32 mL of *tert*-butyl alcohol, 1.07 g (10.56 mmol) of triethylamine, and 3.48 g (12.67 mmol) of diphenylphosphonic azide, and the solution was heated at reflux for 24 h. The solvent was removed under reduced pressure, affording a solid which was dissolved in 50 mL of $CHCl_3$. This solution was washed with 2 M citric acid (3 × 20 mL), 5 % sodium bicarbonate (3 × 30 mL), and water (2 × 20 mL). The organic layer was dried over anhydrous $MgSO_4$ and concentrated to afford a pale yellow solid. The crude gave 2.96 g (79% yield) of pure carbamate **20** upon recrystallization from 40 mL of a EtOH/water (3:1) mixture: mp 88–89 °C; ^{1}H NMR ($CDCl_3$) δ 8.17 (m, 1 H, Ar-3 *H*), 8.09 (m, 2 H, Ar-1,9 *H*), 7.57 (dd, J = 7.7 Hz, J = 1.1 Hz, 1 H, Ar-7 *H*), 7.51 (bs, 1 H, N*H*), 7.35 (m, 2 H, Ar-2,8 *H*), 4.49 (q, J = 7.1 Hz, 2 H, $-OCH_2CH_3$), 1.57 (s, 9 H, *t*-Bu), 1.49 (t, J = 7.1 Hz, 3 H, $-OCH_2CH_3$); ^{13}C NMR ($CDCl_3$) δ 164.64, 154.62, 152.64, 145.51, 129.00, 126.38, 125.58, 124.62, 123.99, 123.10, 122.67, 116.75, 115.53, 114.05, 80.95, 61.22, 20.33, 14.29; MS m/z (M^+) calcd 355.1420, obsd 355.1406.

Hydrolysis 20 Affords 21. A 10-mL round-bottomed flask was charged with 0.22 g (0.62 mmol) of **20**, 0.04 g (1.00 mmol) of NaOH, and 5 mL of methanol, and the solution was heated at reflux for 2 h. After the solvent was removed under reduced pressure, the residue was dissolved in 20 mL of water and the solution was acidified using 6 mL of 2 M citric acid. The suspended solid was isolated by filtration and dried under vacuum to afford 0.20 g (99% crude yield) of crude carbamate acid **21**, which was employed in peptide synthesis and in the preparation of amide derivatives without further purification.

General Methods for Synthesis of Simple Amide Derivatives of 1, 2, and 3. All syntheses were carried out in reagent grade CH_2Cl_2 or anhydrous DMF. Diethylamine and isobutylamine were purified by distillation from KOH. The Bop reagent ((Benzotriazol-1-yloxy)tris-(dimethylamino)phosphonium hexafluorophosphate) was purchased from Richelieu Biotechnologies Inc. and was handled in a fume hood. The hexamethylphosphoric triamide (HMPA) (*CAUTION!* Known carcinogen.) resulting from couplings with the Bop reagent was removed by extraction with 5% acetic acid in water. Removal of the *tert*-butyloxycarbonyl (*t*-Boc) protecting group was carried out by treating the Boc-amino acid with a 25–50% trifluoroacetic acid (TFA) solution in CH_2Cl_2 for 1 h. After concentration under reduced pressure, the remaining TFA in the deprotected material was removed by treatment with Amberlyst A-21 (Aldrich). The A-21 resin (5 mmol of tertiary amine/g of dry resin) was washed with ethanol and CH_2Cl_2 followed by air drying prior to use. All amide derivatives were purified by preparative HPLC as described earlier.

Synthesis of Diamide 27. A 10-mL round-bottomed flask was charged with 0.88 g (1.6 mmol) of pentafluorophenyl ester **9** and 5 mL of CH_2Cl_2. The solution was cooled to 0 °C, and 0.73 g (10 mmol) of isobutylamine was added. After it was stirred for 1.5 h at room temperature, the reaction mixture was diluted with CH_2Cl_2 (50 mL) and washed with 1 M citric acid (3 × 40 mL) and 5% K_2CO_3 (3 × 40 mL). The organic layer was dried ($MgSO_4$) and concentrated to afford 0.65 g (93%) of **22** as a white powder.

A dry 10-mL round-bottomed flask was charged with 0.65 g (1.48 mmol) of **22**, 0.33 g (2.22 mmol) of sodium iodide, 5 mL of dry acetonitrile, and 0.24 g (2.22 mmol) of (TMS)Cl. After 24 h, the mixture was diluted with methanol and stirred for 10 min and the solvent was removed under reduced pressure. The resulting oil was dissolved in 20 mL of CH_2Cl_2, to which was added 50 mL of acetic anhydride and 3 mL of TEA. After 2 h, the solvent was removed under reduced pressure to afford a white powder. This solid was suspended in 100 mL of boiling ethyl acetate/hexanes (6:4). Pure **27** crystallized upon standing overnight to afford 0.35 g (65 % yield): IR (1.5 mM in CH_2Cl_2, cm^{-1}) 3447, 3336, 1660, 1522; ^1H NMR ($CDCl_3$) δ 7.81 (m, 2 H, Ar-1,9 *H*), 7.28 (m, 4 H, Ar-2,3,7,8 *H*), 7.05 (bs, 1 H, N*H*), 5.75 (bs, 1 H, N*H*), 3.71 (q, J = 6.2 Hz, 2 H, $ArCH_2CH_2NH$), 3.33 (t, J = 6.1 Hz, 2 H, $ArCH_2CH_2$), 3.22 (t, J = 6.9 Hz, 2 H, $ArCH_2CH_2$), 3.08 (t, J = 6.0 Hz, 2 H, $HNCH_2CH$), 2.81 (t, J = 5.9 Hz, 2 H, $ArCH_2CH_2$), 1.92 (s, 3H, CH_3CO), 1.77 (m, J = 6.6 Hz, 1 H, $CH(CH_2)_2$), 0.87 (d, J = 6.7 Hz, 6 H, $CH(CH_3)_2$); MS m/z (M^+) calcd 380.2100, obsd 380.2083.

Synthesis of Diamide 28. Diamide **28** was prepared using the same procedure as that used for amide **27** except that diethylamine replaced isobutylamine. The pale yellow oil resulting from the acetylation reaction was suspended in 50 mL of boiling hexanes, to which ethyl acetate was added until the oil dissolved. The solvent mixture was allowed to slowly evaporate to afford 0.30 g (54% yield) of **28** as a white solid: IR (1.5 mM in CH_2Cl_2, cm^{-1}) 3444, 1674, 1633, 1516; ^1H NMR ($CDCl_3$) δ 7.80 (m, 2 H, Ar-1,9 *H*), 7.28 (m, 4 H, Ar-2,3,7,8 *H*), 5.98 (s, 1 H, N*H*), 3.69 (q, J = 6.2 Hz, 2 H, $ArCH_2CH_2NH$), 3.40 (q, J = 7.1 Hz, 4 H, NCH_2CH_3) 3.29 (t, J = 7.3 Hz, 2 H, $ArCH_2CH_2$), 3.19 (t, J = 6.7 Hz, 2 H, $ArCH_2CH_2$), 2.79 (t, J = 7.6 Hz, 2 H, $ArCH_2CH_2$), 1.92 (s, 3H, CH_3CO), 1.10 (td, J = 5.7 Hz, 1.4 Hz, 6 H, CH_3CH_2); MS m/z (M^+) calcd 380.2100, obsd 380.2094.

Synthesis of Diamide 29. A 50-mL round-bottomed flask was charged with 0.39 g (1.02 mmol) of carbamate ester **14**, 0.06 g (1.53 mmol) of NaOH, and 20 mL of methanol. The solution was heated at reflux for 2 h, and the solvent was removed under reduced pressure to afford a solid which was dissolved in 50 mL of water and acidified with 10 mL of 2 M citric acid. The resulting slurry was extracted with $CHCl_3$ (3 × 10 mL), and the organic layer was dried ($MgSO_4$) and concentrated to give crude *N*-Boc protected acid **15**. A dry 50-mL round-bottomed flask was charged with the crude **15**, 0.54 g (1.22 mmol) of Bop reagent, 0.60 g (8.16 mmol) of isobutylamine, and 14 mL of CH_2Cl_2. The solution was then stirred at room temperature for 12 h, and the solvent was removed under reduced pressure to afford a solid which was dissolved in 50 mL of $CHCl_3$. The organic layer was washed with 1 M citric acid (3 × 10 mL) and 5% $NaHCO_3$ (3 × 10 mL), dried, and concentrated to afford 0.37 g of Boc-protected isobutylamide **24**. Removal of *t*-Boc group by TFA solution followed by acetylation with acetic anhydride gave a pale yellow oil as crude **29**. Purification by preparative C_{18} HPLC yielded 0.18 g (65% yield) of diamide **29** as a white solid: mp 254–255 °C; ^1H NMR ($CDCl_3$) δ 7.86 (m, 2 H, Ar-1,9 *H*), 7.61 (m, 4 H, Ar-2,3,7,8 *H*), 6.45 (bs, 1 H, N*H*), 6.22 (bs, 1 H, N*H*), 4.80 (d, J = 6.0 Hz, 2 H, Ar-CH_2NH), 3.85 (s, 2 H, $ArCH_2CO$), 3.04 (t, J = 6.4 Hz, 2 H, $-NCH_2CH(CH_3)_2$), 2.05 (s, 3 H, $-COCH_3$), 1.72 (m, 1 H, $-CH(CH_3)_2$), 0.76 (d, J = 6.7 Hz, 6 H, $-CH(CH_3)_2$); ^{13}C NMR ($CDCl_3$) δ 170.05, 169.94, 154.11, 128.48, 126.95, 124.50, 123.50, 123.10, 122.35, 120.39, 119.89, 119.71, 47.12, 38.80, 38.45, 28.36, 23.40, 19.94; IR (1.5 mM in CH_2Cl_2, CaF_2 cell) 3442, 3351, 1671, 1606 cm^{-1}; MS m/z (M^+) calcd 352.1787, obsd 352.1779.

Synthesis of Diamide 30. Substituting diethylamine for isobutylamine in the procedure outlined above for the synthesis of diamide **29** affords diamide **30** as a crude pale yellow oil. Purification by preparative C_{18} HPLC purification afforded 0.18 g (50% yield) of diamide **30** as a white solid: mp 258–259 °C; ^1H NMR ($CDCl_3$) δ 7.67 (m, 2 H, Ar-1,9 *H*), 7.17 (m, 5 H, Ar-2,3,7,8 *H* and N*H*), 4.61 (d, J = 5.7 Hz, 2 H, Ar-CH_2NH), 3.87 (s, 2 H, $ArCH_2CO$), 3.30 (m, 4 H, $-NCH_2CH_3$), 1.91 (s, 3 H, $-COCH_3$), 1.03 (t, J = 6.9 Hz, 6 H, $-CH_2CH_3$); ^{13}C NMR ($CDCl_3$) δ 170.54, 169.37, 154.12, 153.75, 127.63, 126.11, 124.18, 123.91, 123.05, 122.86, 122.22, 119.69, 119.55, 119.32, 42.51, 40.36, 38.18, 34.58, 22.85, 14.19, 12.96; IR (1.5 mM in CH_2Cl_2, CaF_2 cell) 3444, 1676, 1634, 1604 cm^{-1}; MS m/z (M^+) calcd 352.1787, obsd 352.1780.

Synthesis of Diamide 31. A 10-mL round-bottomed flask was charged with 0.22 g (0.62 mmol) of **20**, 0.04 g (1.00 mmol) of NaOH, and 5 mL of methanol, and the solution was heated at reflux for 2 h. After the solvent was removed under reduced pressure, the residue was dissolved in 20 mL of water and the solution was acidified using 6 mL of 2 M citric acid. The suspended carbamate acid **21** was isolated by filtration and dried under vacuum.

Crude **21** was transferred to a dry 10-mL round-bottomed flask containing 0.41 g (0.93 mmol) of Bop reagent, 0.36 g (4.96 mmol) of isobutylamine, and 5 mL of CH_2Cl_2. The solution was stirred at room temperature for 12 h. The solvent was removed under reduced pressure and the resulting solid was dissolved in 75 mL of $CHCl_3$. The organic layer was then washed with 1 M citric acid (3 × 5 mL) and 5% $NaHCO_3$ (3 × 5 mL), dried, and concentrated to afford 0.32 g of crude carbamate–amide **26**. Removal of the *t*-Boc group using a TFA solution followed by acetylation with acetic anhydride gave a pale yellow solid. Purification by preparative C_{18} HPLC afforded 0.14 g (70% yield) of diamide **31** as a white solid: mp 233–235 °C; ^1H NMR ($CDCl_3$) δ 8.16 (bs, 1 H, N*H*), 8.00 (m, 1 H, Ar-3 *H*), 7.89 (m, 2 H, Ar-1,9 *H*), 7.57 (d, J = 7.7 Hz, 1 H, Ar-7 *H*), 7.47 (bs, 1 H, N*H*), 7.27 (m, 2 H, Ar-2,8 *H*), 3.39 (t, J = 6.6 Hz, 2 H, $-NHCH_2CH(CH_3)_2$), 2.29 (s, 3 H, $-COCH_3$), 2.00 (m, 1 H, $-CH(CH_3)_2$), 1.06 (d, J = 6.6 Hz, 6 H, $-CH(CH_3)_2$); ^{13}C NMR ($CDCl_3$) δ 168.73, 164.09, 152.18, 146.56, 128.25, 124.68, 123.88, 123.82, 123.68, 123.23, 122.76, 120.90, 118.38, 116.71, 47.28, 28.42, 24.04, 20.30; IR (1.5 mM in CH_2Cl_2, CaF_2 cell) 3446, 1734, 1674 cm^{-1}; MS m/z (M^+) calcd 324.1474, obsd 324.1481.

Synthesis of Amide 32. Removal of the *t*-Boc group from 0.70 g (2.15 mmol) of carbamate ester **14** using TFA solution in CH_2Cl_2 (as described above) gave a light yellow oil. Acetylation of the amine by acetic anhydride afforded 0.79 g of light yellow solid. Purification by preparative C_{18} HPLC afforded 0.66 g (95% yield) of pure amide **32** as a white solid: mp 155–156 °C; ^1H NMR ($CDCl_3$) δ 7.84 (m, 2 H, Ar-1,9 *H*), 7.32 (m, 4 H, Ar-2,3,7,8 *H*), 6.30 (bs, 1 H, N*H*), 4.78 (d, J = 5.7 Hz, 2 H, Ar-CH_2NH), 4.16 (q, J = 7.2 Hz, 2 H, $-OCH_2CH_3$), 3.98 (s, 2 H, $ArCH_2CO$), 2.03 (s, 3 H, $-COCH_3$), 1.25 (t , J = 7.2 Hz, 3 H, $-OCH_2CH_3$); ^{13}C NMR ($CDCl_3$) δ 170.81, 170.05, 154.50, 154.14, 128.28, 126.76, 124.40, 124.13, 123.12, 123.09, 122.15, 120.08, 119.87, 118.30, 61.05, 38.80, 35.64, 23.19, 14.19; IR (1.5 mM in CH_2Cl_2, CaF_2 cell) 3444, 3426, 1701, 1665, 1605 cm^{-1}; MS m/z (M^+) calcd 325.1314, obsd 325.1315.

Synthesis of Imide 35. Crude Boc-protected isobutylamide **24** (0.48 g) was deprotected with 10 mL of 30% TFA/CH_2Cl_2 solution and neutralized by treating with Amberlyst A-21 as described above. The crude neutralized brown oil was then stirred with 0.50 g (5.00 mmol) of succinic anhydride, 3 mL of DIEA, and 30 mL of CH_2Cl_2 for 8 h. The solvent was removed under reduced pressure, and the remaining solid was dissolved in 200 mL of 2 N NaOH. Insoluble impurities were isolated by filtration, and the filtrate was acidified with concentrated HCl to afford a white suspension. Filtration followed by drying under reduced pressure yielded 0.41 g of amidic acid **33**. The solid was then heated with 50 mL of acetic anhydride and 0.5 g (6.10 mmol) of anhydrous sodium acetate at 100 °C for 5 h. The solvent was removed under reduced pressure, affording a solid which was extracted with 50 mL of CH_2Cl_2. The organic layer was washed with 5% $NaHCO_3$ (3 × 10 mL), dried, and concentrated to afford a light brown solid as a crude imide. Purification by preparative C_{18} HPLC yielded 0.35 g (71% yield from carbamate ester **14**) of imide **35** as a white solid: mp 163–164 °C; ^1H NMR ($CDCl_3$) δ 7.86 (m, J = 7.6 Hz, 2 H, Ar-1,9 *H*), 7.52 (m, J = 7.6 Hz, 2 H, Ar-3,7 *H*), 7.32 (m, 2 H, Ar-2,8 *H*), 6.90 (bs, 1 H, N*H*), 5.02 (s, 2 H, Ar-CH_2NH), 3.83 (s, 2 H, ArCH_2CO), 3.07 (t, J = 6.2 Hz, 2 H, -NCH_2CH(CH_3)$_2$), 2.75 (s, 4 H, imide methylene *H*), 1.77 (m, 1 H, -C*H*(CH_3)$_2$), 0.81 (d, J = 6.6 Hz, 6 H, -CH(CH_3)$_2$); ^{13}C NMR ($CDCl_3$) δ 177.28, 170.46, 154.73, 154.30, 129.16, 129.07, 125.23, 124.28, 124.05, 123.49, 121.43, 120.49, 120.11, 119.59, 47.73, 38.92, 38.97, 28.94, 28.76, 20.53; IR (1.5 mM in CH_2Cl_2, CaF_2 cell) 3444, 1706, 1669, 1530 cm^{-1}; MS m/z (M^+) calcd 392.1736, obsd 392.1744.

Synthesis of Imide 36. Imide **36** was prepared using the same procedure as that used for imide **35** except that the synthesis commenced from amide **22**. Purification by preparative C_{18} HPLC yielded 0.30 g (60% yield from carbamate ester **9**) of imide **36** as a white solid: mp 128–129 °C; ^1H NMR ($CDCl_3$) δ 7.81 (m, 2 H, Ar-1,9 *H*), 7.29 (m, 4 H, Ar-2,3,7,8 *H*), 7.02 (bs, 1 H, N*H*), 3.98 (t, J = 7.7 Hz, 2 H, ArCH$_2$CH_2N), 3.31 (m, 4 H, ArCH_2CH$_2$), 3.07 (t, J = 6.4 Hz, 2 H, -NCH_2CH(CH_3)$_2$), 2.75 (t, J = 8.1 Hz, ArCH$_2$CH_2CO), 2.62 (s, 4 H, imide methylene *H*), 1.72 (m, 1 H, -C*H*(CH_3)$_2$), 0.84 (d, J = 6.6 Hz, 6 H, -CH(CH_3)$_2$); ^{13}C NMR ($CDCl_3$) δ 177.63, 173.44, 155.11, 128.69, 128.33, 125.33, 124.79, 124.52, 123.56, 123.40, 121.77, 120.05, 119.46, 47.53, 39.00, 36.94, 28.95, 28.86, 28.58, 20.63; IR (1.5 mM in CH_2Cl_2, CaF_2 cell) 3450, 1703, 1663, 1534 cm^{-1}; MS m/z (M^+) calcd 420.2049, obsd 420.2034.

Synthesis of Diamide 38. A 10-mL round-bottomed flask was charged with 2.4 mmol of **37** (Boc protected **1**), 7 mL of THF, 1 mL of DMF, and 2.7 g (19.2 mmol) of methyl iodide. Then 0.17 g (7.2 mmol) of NaH (as a dispersion in paraffin) was added. After it was stirred for 36 h, the heterogeneous mixture was poured into 50 mL of 1 M citric acid (cold) and extracted with CH_2Cl_2 (3 × 25 mL). The organic layer was dried ($MgSO_4$) and concentrated to afford 1.27 g of a pale yellow oil. The crude reaction mixture was heated at reflux in 10 mL of EtOH containing 3.6 mmol of NaOH for 2 h. After the usual citric acid workup, a pale yellow oil was obtained.

The isobutylamide group was introduced into the crude N-methylated acid using 1.1 g (2.49 mmol) of Bop reagent in 20 mL of CH_2Cl_2 containing 1.85 g (25 mmol) of isobutylamine. After the mixture was stirred overnight, the solvent was removed under reduced pressure and the resulting oil was dissolved in 50 mL of ether. The ether layer was washed with 1 M citric acid, 5% acetic acid, and 5% K_2CO_3, dried, and concentrated to afford 1.13 g of a pale yellow solid. After TFA removal of the Boc group and acetylation, a portion of the crude was flash chromatographed ($CHCl_3$/MeOH/HOAc 99:0.5:0.5) to afford 0.85 g of a pale yellow oil. This sample was dissolved in 5 mL of MeOH and further purified by preparative C_{18} HPLC to afford 0.41 g of pure **38** as a white solid: 400-MHz ^1H NMR ($CDCl_3$) (mixture of *E* and *Z* isomers) δ 8.50 and 7.35 (bs, 1 H, N*H*), 7.72 (m, 2 H, Ar-1,9 *H*), 7.19 (m, 4 H, Ar-2,3,7,8 *H*), 3.72 and 3.63 (m, 2 H, ArCH$_2$CH_2NCH$_3$), 3.18 (m, 4 H, ArCH_2CH$_2$), 2.98 and 2.72 (t, J = 6.1 Hz, 2 H, HNCH_2CH(CH_3)$_2$), 2.92 and 2.81 (s, 3H, CH_3N), 2.87 (m, 2 H, ArCH$_2$CH_2CO), 1.95 and 1.61 (s, 3 H, COCH_3), 1.68 and 1.50 (m, 1 H, C*H*(CH_3)$_2$), 0.76 and 0.60 (d, J = 6.6 Hz, 6 H, CH(CH_3)$_2$); IR (1.5 mM in CH_2Cl_2, cm^{-1}) 3446, 3321, 1661, 1653, 1635, 1557, 1541, 1521; MS m/z (M^+) calcd 394.2256, obsd 394.2229.

FT-IR and Variable-Temperature NMR Studies. All amide derivatives studied by FT-IR and VT-NMR were dried under high vacuum in the presence of KOH for 2 days prior to use. The dichloromethane for IR studies was freshly distilled from calcium hydride. The CD_2Cl_2 used for NMR studies was purchased from Aldrich. The concentration of all amides was 1.5 mM. IR spectra were collected on a Galaxy 6021 spectrometer using a CaF_2 solution cell with an optical pathlength of 3 mm. Variable-temperature NMR measurements were performed on a Varian XL-400 spectrometer using residual $CHDCl_2$ (5.32 ppm) as the chemical shift reference at all temperatures.

Synthesis of Peptides. Manual solid-phase peptide synthesis was carried out by employing the benzhydrylamine resin available from Advanced Chemtech having a loading of 0.66 mequiv/g. The dichloromethane, isopropyl alcohol (IPA), and dimethylformamide (DMF) used were reagent grade. DMF was stored over 4-Å molecular sieves to reduce the primary and secondary amine impurities. Side-chain-protected Boc-amino acids were purchased from Advanced Chemtech. Trifluoroacetic acid (TFA) was purchased from PCR Fluorochemicals and was used as a 25–50% solution in CH_2Cl_2 containing 1% thioanisole (Aldrich) as a scavenger. Diisopropylethylamine (DIEA) was dried as described earlier.

The first amino acid was loaded onto the resin by shaking 1.6 equiv of diisopropylcarbodiimide activated amino acid with benzhydrylamine resin for 24 h in CH_2Cl_2. The resin was washed with DMF (2 × 1 min), CH_2Cl_2 (1 × 1min), IPA (1 × 1 min), CH_2Cl_2 (2 × 1 min), IPA (1 × 1 min), and CH_2Cl_2 (4 × 1 min). The completion of the coupling was monitored by the Kasier ninhydrin test. If the result was slightly positive, the remaining unreacted amino groups on the resin were then capped by acetylation. The following cycle was used for each coupling: TFA prewash (25–50% TFA × 1 min), TFA deprotection (25–50% TFA × 50 min), CH_2Cl_2 (2 × 1 min), IPA (1 × 1 min), CH_2Cl_2 (2 × 1 min), IPA (1 × 1 min), CH_2Cl_2 (4 × 1 min), preneutralization (12% DIEA × 1 min), neutralization (12% DIEA × 9 min), coupling (3 equiv of amino acid, 3 equiv of Bop, 4 equiv of DIEA in CH_2Cl_2 containing 10–15% DMF for 2–8 h), DMF (2 × 1 min), CH_2Cl_2 (1 × 1 min), IPA (1 × 1 min), CH_2Cl_2 (2 × 1 min), IPA (1 × 1 min), and CH_2Cl_2 (4 × 1 min). Each coupling step was monitored by the Kasier ninhydrin test. In the case of peptide A and related peptides, the pentafluorophenyl active ester was employed to incorporate amino acid **1** into the peptide. The coupling was performed by shaking the preneutralized resin with 3 equiv of active ester and 3 equiv of DIEA in CH_2Cl_2 overnight. Residues **2** and **3** were coupled to the growing peptide chain using Bop activation of **15** and **21**, respectively.[35] The *t*-Boc-protected amino acids **15** and **21** were prepared before incorporation by hydrolysis of **14** and **20**, respectively, using methodology described in the synthesis of diamide **31**. After the completion of each sequence, the resin-bound peptides were treated with TFA to remove the Boc group, dried under vacuum, and finally cleaved from the resin and side chain deprotected by HF.[24] The crude peptides were purified by preparative HPLC as described earlier. All peptides were characterized by matrix-assisted laser desorption/ionization time-of-flight mass spectroscopy (MALDI-TOFMS)[25] and amino acid analysis. Amino acid analysis (AAA) was performed using a Picotag system. The peptides were hydrolyzed at 110 °C for 24 h in 50:50 (v/v) propionic/hydrochloric acid solution (Pierce) containing 0.2% phenol prior to HPLC analysis.

Summary of Purification and Characterization of Peptides A-K. Peptide A ($C_{51}H_{82}N_{10}O_8$). Purification by preparative C_{18} HPLC employing a linear gradient from 35% to 50% solvent B over 20 min: overall yield 64%; MALDI-TOFMS (MH^+) calcd 964.3, obsd 964.1; AAA Leu 2.0 (2), Lys 1.2 (2), Val 1.9 (2).

Peptide B ($C_{49}H_{78}N_{10}O_8$). Purification by preparative C_{18} HPLC employing a linear gradient from 20% to 46% solvent B over 18 min: overall yield 35%; MALDI-TOFMS (MH^+) calcd 935.6, obsd 936.2; AAA Leu 2.0 (2), Lys 1.1 (2), Val 2.1 (2).

Peptide C ($C_{47}H_{74}N_{10}O_8$). Purification by preparative C_{18} HPLC employing a linear gradient from 15% to 55% solvent B over 23 min: overall yield 41%; MALDI-TOFMS (MH^+) calcd 907.6, obsd 907.6; AAA Leu 2.0 (2), Lys 1.5 (2), Val 2.0 (2).

Peptide D ($C_{48}H_{83}N_{11}O_8$). Purification by preparative C_{18} HPLC employing a linear gradient from 20% to 50% solvent B over 20 min: overall yield 35%; MALDI-TOFMS (MH^+) calcd 942.6, obsd 942.0; AAA Leu 2.0 (2), Lys 1.5 (2), Val 2.0 (2), Pro 1.0 (1), Phe 0.9 (1).

Peptide E ($C_{51}H_{82}N_{10}O_8$). Purification by preparative C_{18} HPLC employing a linear gradient from 20% to 60% solvent B over 20 min: overall yield 53%; MALDI-TOFMS (MH^+) calcd 963.6, obsd 963.6; AAA Leu 1.8 (2), Lys 1.2 (2), Val 2.0 (2).

Peptide F ($C_{51}H_{82}N_{10}O_8$). Purification by preparative C_{18} HPLC employing a linear gradient from 15% to 60% solvent B over 23 min: overall yield 61%; MALDI-TOFMS (MH^+) calcd 963.6, obsd 963.6; AAA Leu 1.9 (2), Lys 1.3 (2), Val 2.0 (2).

Peptide G ($C_{49}H_{78}N_{10}O_8$). Purification by preparative C_{18} HPLC employing a linear gradient from 20% to 60% solvent B over 20 min: overall yield 27%; MALDI-TOFMS (MH^+) calcd 935.6, obsd 935.6; AAA Leu 2.0 (2), Lys 1.3 (2), Val 1.0 (1), Ala 1.0 (1).

(35) (a) Fournier, A.; Wang, C. T.; Felix, A. M. *Int. J. Pept. Protein Res.* **1988**, *31*, 86. (b) Castro, B.; Dormay, J. R.; Evin, G.; Selve, C. *Tetrahedron Lett.* **1975**, 1219.
(36) This figure was prepared with MolScript, see: Kraulis, P. T. *J. Appl. Crystallogr.* **1991**, *24*, 946.
(37) Canary, J. W. Ph.D. Thesis, University of California, Los Angeles, 1988.

Peptide H ($C_{46}H_{72}N_{10}O_8$). Purification by preparative C_{18} HPLC employing a linear gradient from 15% to 60% solvent B over 20 min: overall yield 31%; MALDI-TOFMS (MH^+) calcd 893.6, obsd 893.5; AAA Leu 1.0 (1), Lys 1.0 (2), Val 1.0 (1), Ala 2.0 (2).

Peptide I ($C_{51}H_{82}N_{10}O_8$). Purification by preparative C_{18} HPLC employing a linear gradient from 20% to 55% solvent B over 23 min: overall yield 61%; MALDI-TOFMS (MH^+) calcd 963.6, obsd 963.6.

Peptide J ($C_{55}H_{82}N_{10}O_8$). Purification by preparative C_{18} HPLC employing a linear gradient from 20% to 60% solvent B over 20 min: overall yield 32%; MALDI-TOFMS (MH^+) calcd 1011.6, obsd 1011.7; AAA Leu 2.0 (2), Lys 1.5 (2), Val 1.0 (1), Phe 1.0 (1).

Peptide K ($C_{58}H_{80}N_{10}O_8$). Purification by preparative C_{18} HPLC employing a linear gradient from 25% to 65% solvent B over 20 min: overall yield 39%; MALDI-TOFMS (MH^+) calcd 1045.6, obsd 1045.7; AAA Leu 1.1 (1), Lys 1.6 (2), Val 1.0 (1), Phe 2.1 (2).

Circular Dichroism Studies. CD spectra were collected on a Jasco J-600 spectropolarimeter using a 1-mm quartz cell. The samples were prepared as stock solutions in 10 mM acetate buffer at pH 4.9 and diluted to 0.2 mM with the same buffer. The concentrations of peptides **A-C** were determined by UV spectroscopy at 282 nm (ϵ = 17 797 cm^{-1} M^{-1}), while the concentration of peptide **D** was calculated based on its mass. The samples were allowed to equilibrate at room temperature over 24 h and degassed prior to performing the CD experiments. CD data were collected at 25 °C using a scan speed of 50 nm/min (slower scan speeds give identical data), a time constant of 0.5 s, and a band width of 1 nm. All spectra were corrected for buffer contributions and presented in units of mean residue ellipticity.[29]

Acknowledgment. We thank the reviewers for their thorough and thoughtful critiques, Professors Dave Giedroc, Tom Baldwin, Lila Gierasch, and Nick Pace for helpful discussions, Timothy Hayes for allowing us to perform HF cleavages in his laboratory, David Russell for providing access to and assistance with MALDI-TOFMS, Donald Darensbourg for providing access to FT-IR facilities, Steve Silber and Robert Espina for their help with the NMR experiments, and Tom Holtzman and Seth Snyder for carrying out the ultracentrifugation studies. We gratefully acknowledge financial support of the Robert A. Welch Foundation, Searle Scholars Program/The Chicago Community Trust (J.W.K.), and the National Institutes of Health MARC Predoctural Fellowship program (N.R.G.) and the Center for Macromolecular Design for maintaining the CD spectrometer.

Supplementary Material Available: Text describing experimental details and tables listing bond lengths, bond angles, and coordinates as well as isotropic and anisotropic displacement factors characteristic of the solid-state structure of amide **38** (9 pages). This material is contained in many libraries on microfiche, immediately follows this article in the microfilm version of the journal, and can be ordered from the ACS; see any current masthead page for ordering information.